OPEN ACCESS

University of BRISTOL

Li, J., Pancost, R. D., Naafs, B. D. A., Yang, H., Zhao, C., & Xie, S. (2016). Distribution of glycerol dialkyl glycerol tetraether (GDGT) lipids in a hypersaline lake system. *Organic Geochemistry*, *99*, 113-124. https://doi.org/10.1016/j.orggeochem.2016.06.007

Peer reviewed version

License (if available):
CC BY-NC-ND

Link to published version (if available):
10.1016/j.orggeochem.2016.06.007

Link to publication record in Explore Bristol Research
PDF-document

This is the author accepted manuscript (AAM). The final published version (version of record) is available online via Elsevier at http://dx.doi.org/10.1016/j.orggeochem.2016.06.007. Please refer to any applicable terms of use of the publisher.

University of Bristol - Explore Bristol Research
General rights

This document is made available in accordance with publisher policies. Please cite only the published version using the reference above. Full terms of use are available:
http://www.bristol.ac.uk/red/research-policy/pure/user-guides/ebr-terms/

# Distribution of glycerol dialkyl glycerol tetraether (GDGT) lipids in a hypersaline lake system

Jingjing Li[a,b,c,d], Richard D. Pancost[b,d], B. David A. Naafs[b,d], Huan Yang[a], Cheng Zhao[c], Shucheng Xie[a*]

[a] *State Key Laboratory of Biogeology and Environmental Geology, School of Earth Sciences, China University of Geosciences, Wuhan 430074, China*

[b] *Organic Geochemistry Unit, Bristol Biogeochemistry Research Centre, University of Bristol, Bristol BS8 1TS,UK*

[c] *State Key Laboratory of Lake Sciences and Environment, Nanjing Institute of Geography and Limnology, Chinese Academy of Sciences, Nanjing 210008, China*

[d] *Cabot Institute, University of Bristol, Bristol BS8 1TH, UK*

* Corresponding author. Tel.: +86 13554116626.

*E-mail address*: xiecug@163.com (S.Xie).

ABSTRACT

Isoprenoid glycerol dialkyl glycerol tetraethers (isoGDGTs) of archaeal origin and branched (br)GDGTs of bacterial origin occur in a diverse range of lacustrine sedimentary environments. They have attracted attention as potential temperature proxies, providing high resolution (palaeo)environmental reconstruction from continental interiors. For this study, the distribution of GDGTs and application of GDGT-based proxies to surface samples from Chaka Salt Lake (China) as well as soils and in-flow river sediments were investigated to assess whether GDGT-based proxies are applicable to this hypersaline lake system. We show that iso- and brGDGTs are present in all sediments and soils from the Chaka Salt Lake system. GDGT-0 and crenarchaeol were generally the two most abundant isoGDGTs, suggesting *Thaumarchaeota* as a major biological source of isoGDGTs. The low ratio of crenarchaeol/crenarchaeol regioisomer suggests that *Thaumarchaeota* of the lake sediments is likely *Thaumarchaeota* group I.1b derived from the surrounding alkaline soils, arguing against the use of the $TEX_{86}$ proxy in this system. Because alkaline soils generally have high isoGDGT concentrations, it is likely that a large allochthonous input of isoGDGTs will be a pervasive challenge to palaeoclimate applications in such settings. On the other hand, the brGDGT distributions in the lake and river sediments differed markedly from those in the surrounding soils, suggesting that instead of deriving from the surrounding soils at least part of the brGDGTs are synthesized *in situ*

or delivered from more distal upland soils. Taken together, our results indicate that the mixed sources of GDGTs in Chaka Salt Lake complicate the application of GDGT-based proxies, and it will be challenging to use such proxies in this system.

Keywords: GDGT; hypersaline; lacustrine; MBT/CBT; $TEX_{86}$

## 1. Introduction

Glycerol dialkyl glycerol tetraethers (GDGTs) are core membrane-spanning lipids synthesized by Archaea and Bacteria. They are ubiquitous in the environment, occurring in marine and lacustrine sediments, and in the water column, soil, peat, hot springs, loess and stalagmites [see Schouten et al. (2013) for a review]. Isoprenoid GDGTs (isoGDGTs) are characterized by two biphytane carbon skeletons with a varying number of cyclopentane moieties, exhibit *sn*–2,3 stereochemistry (Fig. 1), and are synthesized by Archaea, including *Euryarchaeota*, *Crenarchaoeota* and *Thaumarchaeota* (Weijers et al., 2007, Pearson and Ingalls, 2013). A specific isoGDGT, crenarchaeol, containing four cyclopentane rings and one cyclohexane ring appears to be synthesized exclusively by *Thaumarchaeota* (formerly Marine Group I Crenarchaeota; Sinninghe Damsté et al., 2002, Pitcher et al., 2010). Branched GDGTs (brGDGTs) are of putative bacterial origin, exhibit *sn*–1,2 stereochemistry and feature methylated alkyl chains containing up to two cyclopentane moieties (Sinninghe Damsté et al., 2000, Weijers et al., 2006). Although the specific biological source of brGDGTs has not been identified, *Acidobacteria* are generally considered to be the likely source organisms because structural characteristics similar to those of brGDGTs were found in the lipids of subdivisions 1, 3 and 4 of this phylum (Peterse et al., 2010, Sinninghe Damsté et al., 2011, 2014).

In recent years, numerous investigations have demonstrated that GDGT-based

61 proxies in both marine and terrestrial sedimentary environments are powerful
62 palaeoenvironmental recorders. $TEX_{86}$ was first established using marine sediments and
63 is based on the distribution of cyclic moieties of isoGDGTs, biosynthesized mainly by
64 aquatic *Thaumarchaeota* (Schouten et al., 2002, Pearson and Ingalls, 2013, Schouten et
65 al., 2013) that are ubiquitous and abundant in marine environments (Karner et al., 2001).
66 Although $TEX_{86}$ was initially developed for the marine environment, the occurrence of
67 *Thaumarchaeota* in lacustrine environments (Keough et al., 2003) led to the
68 development of several global and regional $TEX_{86}$ lake calibrations (Blaga et al., 2009,
69 Powers et al., 2010, Castañeda and Schouten, 2011). Application of $TEX_{86}$ to lakes has
70 generated lake water temperature values consistent with other approaches, suggesting
71 that it can be applied to certain lacustrine systems to provide a new proxy for
72 continental palaeotemperature change (Tierney et al., 2008, 2010a, Woltering et al.,
73 2011, Berke et al., 2012, Blaga et al., 2013). However, its application to some lakes has
74 resulted in unreliable temperature estimates, presumably because the sediments
75 contained isoGDGTs derived from other sources such as methanotrophs or non-aquatic
76 *Thaumarchaeota* (Blaga et al., 2009, Pearson et al., 2011, Naeher et al., 2012,
77 Sinninghe Damsté et al., 2012a, Naeher et al., 2014).

78 The methylation of branched tetraethers (MBT) and cyclization of branched
79 tetraethers (CBT) indices were initially based on the analysis of brGDGTs in a global
80 soil database (Weijers et al., 2007) (see Fig. 1 for GDGT structures). That work

81 revealed that the distribution of brGDGTs in soil is strongly influenced by temperature
82 and soil pH (Weijers et al., 2007, Peterse et al., 2012). The widespread occurrence of
83 brGDGTs in lakes suggested that the proxy could also be applied to these systems
84 (Blaga et al., 2009, Bechtel et al., 2010, Tierney et al., 2010b, Pearson et al., 2011,
85 Wang et al., 2012). However, subsequent work suggested that the transfer functions
86 originally developed for soils could systematically underestimate the actual temperature,
87 as shown for some European and American lakes (Blaga et al., 2010), East African
88 lakes (Tierney et al., 2010b), and Lake Lochnagar in Scotland (Tyler et al., 2010). This
89 reflects two factors. First, brGDGT distributions differ between soil and lake sediment
90 (Sinninghe Damsté et al., 2009, Tierney and Russell, 2009) and second, brGDGTs are
91 evidently produced within lakes, either in the water column or in the lake sediment,
92 making it unclear whether brGDGTs in a given setting arise from allochthonous (soil)
93 input or *in situ* production (Tierney et al., 2010b, Loomis et al., 2011, Sinninghe
94 Damsté et al., 2012a, Wang et al., 2012, Schoon et al., 2013). On this basis, several
95 studies have attempted to generate regional and global lake-specific MBT(')/CBT
96 temperature calibrations (Tierney et al., 2010b, Pearson et al., 2011, Sun et al., 2011,
97 Loomis et al., 2012, Günther et al., 2014). Reconstructed temperatures based on these
98 lake-specific calibrations are in good agreement with instrumental values and/or other
99 proxy records (D'Anjou et al., 2013, Peterse et al., 2014), although some discord
100 between estimated and actual temperatures remains (Niemann et al., 2012, Sinninghe

Damsté et al., 2012a). Hence, the mixed sources of brGDGTs in lake environments complicate their application, and more details about their distribution are required before applying them as palaoenvironmental recorders.

Although many studies have focussed on GDGTs in lacustrine settings (Blaga et al., 2009, Bechtel et al., 2010, Das et al., 2012, Wang et al., 2012, Schoon et al., 2013, Naeher et al., 2014, Peterse et al., 2014), only a few studies have examined hypersaline lake systems (Günther et al., 2014, Huguet et al., 2015). In particular, very few studies have examined brGDGTs in hypersaline lakes. We have therefore investigated the distribution and concentration of GDGTs in sediments from a hypersaline lake system (Chaka Salt Lake), as well as in inflow river sediments and soil samples collected in the catchment to the west of the lake (Fig. 2). The lake was selected because its salinity is about 10x average seawater salinity (Zheng et al., 2002). In addition, microbial data are available for the lake (Jiang et al., 2006, 2007, Yang et al., 2013), which could help to support the identification of the biological source(s) of GDGTs. Moreover, the lake is not of marine origin but evolved from an inland freshwater lake, which makes it an excellent site for studying the behaviour of GDGTs in hypersaline lacustrine environments.

## 2. Material and methods

### *2.1. Study site*

Chaka Salt Lake (36°38'–36°46'N, 99°01'–99°12'E) is an athalassohaline lake (a saline lake not of marine origin) 3200 m above sea level in the southeastern edge of Qaidam Basin in northwestern China (Fig. 2). It is located between Nanshan Mountain on the northern side and Ela Mountain on the southern side. Salinity ranges between 317 and 347 psu. The area of the lake covers 105 $km^2$, with a catchment area of ca. 11,600 $km^2$. It is a hydrologically half open drainage basin with no outflow, but is fed by two freshwater rivers: Mo River and Hei River. In addition, fresh water springs feed into the lake on its northeastern and southeastern bank (Fig. 2). Local meteorological data (http://cdc.nmic.cn/home.do) indicate that the lake and surrounding area are characterized by a dry continental climate. The mean annual temperature is 5.0 °C, with the lowest mean monthly temperature of –11.2 °C in January and the highest of 19.8 °C in July. The mean temperature for summer and winter is 18.6 °C and –9.2 °C, respectively. Annual precipitation (210 mm) is greatly exceeded by evaporation (2,000 mm), causing the high salinity of the lake. The water depth is > 50 cm during the rainy season (June, July and August) and decreases to 1 cm during the dry season (January, February and March). The average lake pH is 7.0 and the pH of water from the Mo and Hei river is 7.0 and 6.8, respectively (Zheng et al., 2002, Liu et al., 2008). The soil pH of the catchment is between 7.9 and 8.4 (national soil database; http://vdb3.soil.csdb.cn/). At the time of sampling (August), the measured temperature of surface water is around 17 °C.

141 The landscape of the study site is dominated by alpine meadows and steppe, the
142 vegetation type is dominated by C3 plant, mainly *Poa* sp., *Kobresia* sp., and *Oxytropis*
143 *ochrocephala* (Duan et al., 2014). Typical soils are calcic brown soils and/or
144 castanozem and all from low-density grassland covered soil.
145
146 *2.2. Sampling and laboratory analysis*
147 Four river surface sediment samples (0-2 cm), six lake surface sediment samples (0-2
148 cm) and five soil samples (0-2 cm) were collected in and around the lake during a field
149 campaign in August 2011 (Fig. 2, Table 1). Samples were freeze-dried and
150 homogenized with a mortar and pestle directly after transport to the laboratory.
151 Elemental and inorganic carbon (IC) were measured using a Carlo Erba EA1108
152 Elemental Analyzer and modified Coulomat 702 analyser, respectively. Total Organic
153 Carbon (TOC) concentration was determined by subtracting the IC content from the
154 total C content. TOC values represent the mean of duplicate measurements.
155 Samples were weighted into tin capsules and introduced into the combustion furnace
156 (1800 °C) flushed with $O_2$. The combustion products were separated using gas
157 chromatography (GC, Porpac Q column) and the composition (%) determined via
158 thermal conductivity detection. IC was measured with a modified Coulomat 702
159 analyser. It was liberated as $CO_2$ using orthophosphoric acid and flushed with $N_2$ into
160 the coulomatic cell set to known pH (9.2), resulting in a decrease in pH. The magnitude

of the current applied to return the cell to its original value is directly proportional to the IC released as $CO_2$.

Lipid extraction generally followed Yang et al. (2012) with some modifications. Each sample (ca. 10 g) was ultrasonically extracted 6x with dichloromethane DCM/MeOH (9:1, v/v). The total lipid extract (TLE) was concentrated using rotary evaporation under vacuum and separated using column chromatography with silica gel as stationary phase and hexane/DCM (9:1, v/v) and DCM/MeOH (9:1, v/v) to yield an apolar and a polar fraction, respectively. The polar fraction, containing the GDGTs, was filtered over a 0.45um PTFE filter with hexane/isopropanol (99:1, v/v) and dried under $N_2$ prior to analysis using high performance liquid chromatography/atmospheric pressure chemical ionisation mass spectrometry (HPLC-APCI-MS).

GDGT analysis was performed with an Agilent 1200 series liquid chromatograph connected to a triple quadrupole mass spectrometer, using single ion monitoring (SIM) mode and *m/z* 1302, 1300, 1298, 1296, 1294, 1292, 1050, 1048, 1046, 1036, 1034, 1032, 1022, 1020, 1018 and 744, 653 to enhance sensitivity. Separation was achieved using an Alltech Prevail Cyano column (150 × 2.1 mm, 3 μm), following the method of Yang et al. (2014). Quantification was obtained by addition of an internal synthetic $C_{46}$ GDGT standard (cf. Huguet et al., 2006). The final quantification was semi-quantitative as we did not determine the relative response factor between GDGTs and the standard. For determination of ACE (see below), the response factors for archaeol and GDGT-0 were

assumed to be identical

*2.3. Calculation of GDGT indices and proxies*

Indices based on the distribution of GDGTs were calculated according to previous studies, $TEX_{86}$ was calculated following the equation of Schouten et al. (2002), the Roman and Arabic numerals correspond to GDGT structures in Fig. 1:

$$TEX_{86} = \frac{GDGT-2 + GDGT-3 + Cren'}{GDGT-1 + GDGT-2 + GDGT-3 + Cren'} \quad (1)$$

The soil input index, BIT was calculated following the equation of Hopmans et al. (2004):

$$BIT = \frac{GDGT-I + GDGT-II + GDGT-III}{GDGT-I + GDGT-II + GDGT-III + Cren} \quad (2)$$

The MBT and CBT indices were calculated as follows (Weijers et al., 2007):

$$MBT = \frac{([I] + [Ib] + [Ic])}{([I] + [Ib] + [Ic] + [II] + [IIb] + [IIc] + [III] + [IIIb] + [IIIc])} \quad (3)$$

$$CBT = -\log\left(\frac{([Ib]+[IIb])}{([I]+[II])}\right) \quad (4)$$

The revised MBT' was calculated according to the equation developed by Peterse et al. (2012):

$$MBT' = \frac{([I] + [Ib] + [Ic])}{([I] + [Ib] + [Ic] + [II] + [IIb] + [IIc] + [III])} \quad (5)$$

The ratio of total isoGDGTs and total brGDGTs index, $R_{i/b}$ was calculated according to the equation of Xie et al. (2012):

$$R_{i/b} = \frac{\sum isoGDGTs}{\sum brGDGTs} \quad (6)$$

The ratio of archaeol and GDGT-0 index, ACE was calculated according to the equation

of Turich and Freeman (2011), except that the multiplication by 100 has been removed to make it more consistent with other GDGT-based indices.

$$\mathrm{ACE} = \frac{\mathrm{archaeol}}{\mathrm{archaeol+GDGT-0}} \quad (7)$$

We note that recent analytical developments have revealed that the pentamethylated and hexamethylated brGDGTs actually comprise multiple structural isomers, with methylation at either C-5 or C-6 (De Jonge et al., 2013).This has resulted in a new soil calibration (De Jonge et al., 2014a) but not new lake calibrations. Here, we applied the original analytical approaches and calibrations, in which C-5 and C-6 isomers are integrated together.

$TEX_{86}$ inferred lake surface temperature (LST) was calculated using Eqs. 8-12 (Powers et al., 2010, Tierney et al., 2010a, Castañeda and Schouten, 2011). Specific calibrations for summer (SLST) and winter lake surface temperature (WLST) were used to infer seasonal temperatures (Powers et al., 2010).

$$\mathrm{LST_{Powers2010}} = 50.8 \times \mathrm{TEX_{86}} - 10.4 \quad (8)$$

$$\mathrm{SLST_{Powers2010}} = 46.6 \times \mathrm{TEX_{86}} - 5.6 \quad (9)$$

$$\mathrm{WLST_{Powers2010}} = 57.3 \times \mathrm{TEX_{86}} - 17.5 \quad (10)$$

$$\mathrm{LST_{Tierney2010}} = 38.87 \times \mathrm{TEX_{86}} - 3.50 \quad (11)$$

$$\mathrm{LST_{Castañeda2011}} = 54.89 \times \mathrm{TEX_{86}} - 13.36 \quad (12)$$

MBT'/CBT inferred mean annual air temperature (MAAT) was calculated for the soil and lake sediments. Based on a globally distributed soil calibration (Weijers et al.,

2007), MAAT can be obtained using Eq. 13. This calibration was extended and revised with a new transfer function (Eq. 14) by Peterse et al. (2012). In addition, new (local) calibrations were proposed by Yang et al. (2014) for semiarid and arid regions of China (Eq. 15 and 16).

$$\mathrm{MAAT}_{\mathrm{Weijers2007}} = (\mathrm{MBT} - 0.12 - 0.19 \times \mathrm{CBT})/0.02 \quad (13)$$

$$\mathrm{MAAT}_{\mathrm{Peterse2012}} = 0.81 - 5.67 \times \mathrm{CBT} + 31.0 \times \mathrm{MBT}' \quad (14)$$

$$\mathrm{MAAT}_{\mathrm{Yang2014}} = 7.5 + 16.1 \times \mathrm{MBT} - 1.2 \times \mathrm{CBT} \quad (15)$$

$$\mathrm{MAAT}_{\mathrm{Yang2014,}} = 20.9 - 13.4 \times f(\mathrm{II}) - 17.2 \times f(\mathrm{III}) - 17.5 \times f(\mathrm{IIb}) + 11.2 \times f(\mathrm{Ib}) \quad (16)$$

All samples were analysed in duplicate and the data are presented as the mean of these duplicates. The average analytical duplicate error for GDGT-based indices was < 0.01.

Several global and regional lake temperature calibration studies have been proposed for African lakes (Tierney et al., 2010b, Loomis et al., 2012), Chinese and Nepalese lakes (Sun et al., 2011) and lakes along a transect from the Scandinavian Arctic to Antarctica (Pearson et al., 2011), in addition the newly developed calibration for Tibetan Plateau (Günther et al., 2014):

$$\mathrm{MAAT}_{\mathrm{Tierney2010}} = 11.8 + 32.5 \times \mathrm{MBT} - 9.3 \times \mathrm{CBT} \quad (17)$$

$$\mathrm{MAAT}_{\mathrm{Tierney2010,}} = 50.5 - 74.2 \times f(\mathrm{III}) - 31.6 \times f(\mathrm{II}) - 34.7 \times f(\mathrm{I}) \quad (18)$$

$$\mathrm{MAAT}_{\mathrm{Sun2011}} = 4.0 + 38.2 \times \mathrm{MBT} - 5.6 \times \mathrm{CBT} \quad (19)$$

241 $$\mathrm{MAAT}_{\mathrm{Pearson2011}} = 20.9 + 98.1 \times f(\mathrm{Ib}) - 12.0 \times f(\mathrm{II}) - 20.5 \times f(\mathrm{III}) \quad (20)$$

242 $$\mathrm{MAAT}_{\mathrm{Loomis2012}} = 2.5 + 45.3 \times \mathrm{MBT} - 5.0 \times \mathrm{CBT} \quad (21)$$

243 $$\mathrm{MAAT}_{\mathrm{Loomis2012'}} = 36.9 - 50.1 \times f(\mathrm{III}) - 35.5 \times f(\mathrm{II}) - 1.0 \times f(\mathrm{I}) \quad (22)$$

244 $$\mathrm{MAAT}_{\mathrm{Günther2014}} = -3.84 + 9.84 \times \mathrm{CBT} + 5.92 \times \mathrm{MBT'} \quad (23)$$

245 where *f* is the fractional abundance of a specific brGDGT relative to total brGDGTs.
246 Note that in the above equations (and below), we use the prime symbol (i.e.
247 $\mathrm{MAAT}_{\mathrm{Tierney2010}}$ and $\mathrm{MAAT}_{\mathrm{Tierney2010'}}$) to indicate calibrations that directly use fractional
248 abundance of brGDGTs as opposed to MBT values.

249

250 **3. Results**

251 *3.1. Concentration and distribution pattern of isoGDGTs*

252 All samples contained isoGDGTs, but the concentration, normalized to total organic
253 carbon (TOC), varied substantially (Table 1 and Fig. 3). The summed concentration
254 (semi-quantitatively determined) in soils ranged from 80 to 1050 ng/g TOC, lower than
255 concentrations in river and lake sediments, which varied from 580 to 2040 ng/g TOC
256 and 60 to 2560 ng/g TOC, respectively. GDGT-0 was generally the most abundant
257 isoGDGT both in river (50–80% of major isoGDGTs) and lake sediments (30–75%),
258 with one exception in sample LS10 where crenarchaeol (33%) was the dominant
259 isoGDGT (Table 1). The concentration of isoGDGTs with cyclopentane(s) moieties
260 (isoGDGT 1-3) was low in most river and lake sediment samples. In river sediments,

261 the relative abundance of crenarchaeol is higher than GDGT-1, GDGT-2 and GDGT-3.
262 In contrast, lake sediments contained more complex distributions (Table 1); for example,
263 crenarchaeol was generally more abundant than isoGDGTs 1-3, but the proportion of
264 GDGT-1 was higher than that of crenarchaeol in samples LS5, LS8 and LS9 (Table 1,
265 Fig. 3). The distribution pattern of isoGDGTs in soils was also variable. Crenarchaeol
266 dominated in samples S11, S12, S14, whereas GDGT-0 was the most abundant in S13
267 and S15 (Table 1, Fig. 3).

268 $TEX_{86}$ values for river sediments and soils were almost identical at 0.68 ± 0.03 and
269 0.69 ± 0.05, respectively (Table 1). The $TEX_{86}$ values for lake sediments show high
270 variability, ranging from 0.28 to 0.72. The ACE index, based on the relative abundance
271 of archaeol and GDGT-0, was determined for river sediments, lake sediments and soils.
272 ACE indices for river sediments and soils are generally lower than those of lake
273 sediments, ranging from 0.01 to 0.18 in river sediment and from 0.01 to 0.14 in soils
274 (Table 1). Indeed, the amount of archaeol in soil sample S14 is quite low, and the ACE
275 index of S14 is close to 0. In contrast, the ACE values of lake sediments are generally
276 higher than river sediments and soils (Table 1), varying from 0.16 to 0.66.

277

278 *3.2. Concentration and distribution pattern of brGDGTs*

279 The concentration of total brGDGTs in river sediments, lake sediments and soils
280 varied from 640-3300 ng/g TOC, 30-1740 ng/g TOC and 20-910 ng/g TOC respectively

(Table 2, Fig. 3). In contrast to the lower concentration of isoGDGTs in soils than sediments, the total concentration of brGDGTs in river samples was higher than in lake sediments and soils. The brGDGTs without cyclopentane moieties (GDGT I, II, and III) were generally more abundant than cyclopentane ring-containing brGDGTs.

MBT indices for river and lake sediments were similar at 0.20 ± 0.02 and 0.16 ± 0.06, respectively. MBT for soils was lower, with values of 0.07 ± 0.01. Due to the low concentration of GDGT-IIIb and –IIIc for all samples, MBT' was almost identical to MBT (Table 2). CBT values were also similar for river and lake sediments at 0.22 ± 0.09 and 0.32 ± 0.23, respectively. CBT for soils was much higher at 1.26 ± 0.20 (Table 2). BIT values for river sediments, lake sediments and soils were 0.77 ± 0.11, 0.68 ± 0.18, and 0.57 ± 0.09, respectively (Table 1) – intriguingly, BIT values are lowest in the soils. The $R_{i/b}$ index for river sediments, lake sediments and soils was 0.95 ± 0.27, 5.75 ± 5.34 and 2.48 ± 1.45, respectively.

## 4. Discussion

### *4.1. Potential biological sources of isoGDGTs*

#### *4.1.1. GDGT-0*

GDGT-0 has a wide range of biological sources. It is produced by all major groups of archaea except for halophilic archaea, although it has been found in halophilic environments (Turich and Freeman, 2011, Schouten et al., 2013). Despite that, the

likely biological sources of GDGT-0 in terrestrial settings appear to be mainly methanogens and *Thaumarchaeota* (Blaga et al., 2009). The ratio of GDGT-0/crenarchaeol has been proposed to evaluate the contribution of GDGT-0 produced by methanogens and a value > 2 is generally thought to reflect a substantial contribution from methanogens to the isoGDGT pool (Blaga et al., 2009, Bechtel et al., 2010). The ratio was generally < 2 for our soil samples (except for one sample S15, Table 1), similar to the value for the catchment soils from other lakes (Naeher et al., 2014), suggesting that GDGT-0 in the surface of soils of our hypersaline lake system is derived mainly from *Thaumarchaeota*. However the ratio was > 6 for S15, indicating that this soil could contain a significant amount of methanogens. The soils span a range of different types of calcic brown soils and/or castanozem, and all come from low-density grassland covered soil, indicating there must be additional factors other than soil type and vegetation type that determine the isoGDGT composition in soils.

The GDGT-0/crenarchaeol ratios in river sediments were much higher than those of the soils, with values between 1.7 and 7.1 (Table 1), suggesting that methanogens were a main source of GDGT-0. In comparison, the ratio in lake sediments was highly variable. For LS6, LS7 and LS10, it varied between 0.9 and 2.2. These values are similar to those for the surrounding soils and river sediments, indicating these lake sediments could contain significant contribution of *Thaumarchaeota*. However, some lake sediments were characterized by much higher ratio values, between 16.3 and 52.4

for LS5, LS8, and LS9. These are similar to those reported from European lake sediments (Blaga et al., 2009) and indicate that methanogens are likely a major source of GDGT-0 in at least some of our lake sediments. These results suggest that there must be some methanogens with high salinity tolerance and which produce GDGT-0 in this hypersaline setting. However, the contribution of other types of halophilic archaea cannot be excluded. Although GDGT-0 has not been detected in cultures of these organisms, uncultured halophiles could be the producers of GDGT-0 in hypersaline settings (Turich and Freeman, 2011, Birgel et al., 2014, Huguet et al., 2015). Indeed, there is an increasing number of studies showing the potential of halophilic archaea to produce biphytanes (see Turich and Freeman (2011) and references therein).

Microbial diversity analyses of water and sediments from the lake demonstrate that the majority of archaeal clone sequences in the sediments are related to methanogens and only a small proportion of sequences was affiliated with the *Crenarchaeota* group (Jiang et al., 2006), probably indicating the contribution of GDGT-0 from *Crenarchaeota* is less than methanogens. The phylogenetic compositions of the archaeal clone libraries of lake water show a distinct difference, all archaeal clone sequences for lake water were related to the *Halobacteriales* group due to high salinity (Jiang et al., 2006). However, only a small percentage of sequences was related to *Halobacteriales* for lake sediments (Jiang et al., 2006), indicating the production of GDGT-0 from uncultured halophiles could not be excluded. Taken together our results indicate that

GDGT-0 in river and lake sediments is derived predominantly from methanogens with high salinity tolerance and allochthonous *Thaumarchaeota* sources.

*4.1.2. Crenarchaeol and crenarchaeol regioisomer*

Crenarchaeol and its regioisomer are considered to be synthesized uniquely by the phylum *Thaumarchaeota* ($NH_4^+$ oxidizing archaea) in aquatic and terrestrial environments including the water column, sediments and soils, and they have been found in all cultures of *Thaumarchaeota* (see Schouten et al., 2013 and references therein). Recent research suggests that it could also be synthesized by Marine Group II *Euryarchaeota* (Lincoln et al., 2014a), but that study is controversial (Lincoln et al., 2014b, Schouten et al., 2014). Several studies have shown that significant quantities of the regioisomer (relative to crenarchaeol) are produced by soil *Thaumarchaeota* group I.1b, in contrast to the low amount normally found in (aquatic) *Thaumarchaeota* group I.1a (Kim et al., 2012, Sinninghe Damsté et al., 2012b). Therefore, we use the ratio of crenarchaeol and its regioisomer (cren/cren') to distinguish the type of *Thaumarchaeota* (Sinninghe Damsté et al., 2012a, Liu et al., 2013). Based on published data, we propose that values >25 are indicative for *Thaumarchaeota* group I.1a and markedly lower ones indicative for group I.1b (Fig. 4, Table A1 in Supplementary material). An overview of reported values shows that cren/cren' in soils is generally much lower than for lake and marine sediments (Fig. 4). The values for our river sediments, lake sediments and soils

361 are similar: 13.3 ± 2.0, 10.2 ± 2.8 and 21.8 ± 6.9, respectively. Interestingly the values
362 in the soils are higher than for the river and lake sediments (Table 1), but are all < 25.
363 This suggests that *Thaumarchaeota* in the Chaka Salt Lake system are dominated by
364 group I.1b *Thaumarchaeota*.

365 As halophiles are not known to produce crenarchaeol or its regioisomer, and the
366 cren/cren' ratios in our lake sediments are similar to those in river sediments and soils,
367 we suggest that in the lake sediments crenarchaeol and its regioisomer derive
368 predominantly from either surrounding soils or riverine input. This is supported by
369 genomic data that indicate that the functional gene encoding for the first step in $NH_4^+$
370 oxidation for *Thaumarchaeota* (*amoA*) was not present in water and sediment samples
371 from Chaka Salt Lake (Yang et al., 2013).

372

373 *4.1.3. IsoGDGT-1 to 3*

374 Significant amounts of isoGDGTs 1-3, containing cyclopentane moieties, were
375 present in all samples. They can derive from both *Thaumarchaeota* and methanogens
376 (and also anaerobic methanotrophs; Pancost et al., 2001, Schouten et al., 2013) and
377 further investigation is required to verify their biological sources. As shown in Fig. 3,
378 the average proportion of GDGT-1, GDGT-2 and GDGT-3 for each setting was similar,
379 although the proportion of GDGT-1 in lake sediments was higher than the other two
380 settings, leading to a relatively low $TEX_{86}$ for lake sediments. Regardless of source, the

381 average proportion of these isoGDGTs is roughly similar in river sediments and soils,
382 suggesting that these isoGDGTs, like crenarchaeol, likely derive from the surrounding
383 soils.
384
385 *4.1.4. Overview of isoGDGT sources*
386 It seems likely that the predominance of isoGDGTs in lake sediments, especially
387 crenarchaeol and isoGDGTs 1-3, are derived from soils. It is likely that this arises from
388 their atypically high concentration in the surrounding soils (Table 1). In fact, the
389 average concentration of crenarchaeol in the soils (260 ng/g TOC) was higher than that
390 in river (230 ng/g TOC) and lake sediments (110 ng/g TOC). This strong crenarchaeol
391 contribution to the soils is evident from their relatively low BIT indices (0.57 ± 0.09)
392 compared to previously investigated soils in which BIT indices are normally >0.9 (see
393 Schouten et al. (2013) and references therein). Although this particular effect could be
394 site-specific, we suggest that it could be characteristic of many hypersaline lake systems,
395 because a relatively high concentration of crenarchaeol and relatively low concentration
396 of brGDGTs is characteristic of arid environments and alkaline soils (Yang et al., 2014).
397
398 *4.2. Potential biological sources of brGDGTs*
399 The distribution of brGDGTs, illustrated for example by a cross plot of MBT and
400 CBT indices (Fig. 5), was markedly different between soils and sediments. The

401 different distribution suggests that there is a contribution of *in situ* produced brGDGTs
402 to the river and lake sediments and that the brGDGTs do not originate solely from the
403 surrounding soils. The average brGDGT concentration for lake sediments is also higher
404 than that for soils (Table 1), further indicating that a significant amount of brGDGTs is
405 produced within Chaka Salt Lake. These results are consistent with those from other
406 river and lake systems where brGDGTs are produced *in situ* (Zell et al., 2013, De Jonge
407 et al., 2014b).

408 GDGT distributions are also consistent with separate lake and soil sources. The
409 distribution of brGDGTs in the sediments is similar to that in lakes from around the
410 world, with GDGT-II dominating (Tierney et al., 2010b, Tyler et al., 2010, Loomis et
411 al., 2011, Pearson et al., 2011, Sun et al., 2011, Schoon et al., 2013, Loomis et al., 2014).
412 In contrast, the most abundant brGDGT in surrounding soils is GDGT-III. This further
413 supports our suggestion that brGDGTs in our lake sediment samples were derived from
414 *in situ* production, either in the lake water column or sediments. However, as discussed
415 above, brGDGT distributions do differ. Although brGDGTs II and III are the most
416 abundant in sediments and soils, in sediments GDGT II is nearly as abundant as GDGT
417 III whereas it is less abundant than GDGT III in soils (Fig. 3). The dominance of GDGT
418 III, followed by GDGT-II and GDGT-I, in soils is similar to that reported for soils from
419 dry and cold regions like high altitude regions in Norway (Peterse et al., 2009), western
420 states from the USA (Dirghangi et al., 2013) and Qinghai-Tibetan Plateau, China (Liu et

al., 2013).

A complication is that microbial ecological analysis of this lake suggested that the majority of bacteria in the water and sediments were *Bacteroidetes* and low G + C gram positive bacteria, respectively (Jiang et al., 2006), and not *Acidobacteria*, a presumed biological source of brGDGTs (Sinninghe Damsté et al., 2011, 2014). This would suggest that either the brGDGTs in sediments from Chaka Salt Lake are derived from riverine sources and/or are produced *in situ* by organisms other than *Acidobacteria*. Moreover, it is not known if the microbial communities differ between the dry and rainy season; although both biomarker and microbial ecology sampling was conducted during the rainy season, it is possible that brGDGTs were generated at another time under different conditions. Further testing is required to differentiate these possibilities.

### *4.3. Implications for application of GDGT proxies*

#### *4.3.1. BIT*

The BIT index was originally developed to trace the input of soil organic matter (OM) to aquatic environments. Values close to 1 (absence of crenarchaeol) are typical for soils, whereas values close to 0 are typical for open marine and large lake sediments (Hopmans et al., 2004). For Chaka Salt Lake the BIT values of river (0.77 ± 0.11) and lake sediments (0.68 ± 0.18) were higher than those of soil (0.57 ± 0.09). Previous studies have shown that the BIT index in soils is influenced by pH, with values

441 decreasing in Chinese soils with pH > 5.5 (Yang et al., 2012); given the high pH values
442 for soils surrounding Chaka Salt Lake, that is likely the explanation here. The
443 predominance of isoGDGTs over brGDGTs in alkaline soils, in contrast to the brGDGT
444 dominance in acid and neutral soils (Yang et al., 2014), is also reflected in higher $R_{i/b}$
445 ratios (Xie et al., 2012).

446 It seems that alkaline soils favor the growth of archaeal community, and especially
447 *Thaumarchaeota* (Bates et al., 2011). Hence, the alkaline conditions in soils from the
448 catchment area of Chaka Salt Lake (with pH around 8), will likely favor the growth of
449 *Thaumarchaeota*, leading to the high amounts of crenarchaeol (and other isoGDGTs)
450 we observe in our samples. Consequently, the limitations of the BIT index are likely
451 relevant for other arid systems – and other hypersaline lakes.

452

453 *4.3.2. $TEX_{86}$*

454 The applicability of $TEX_{86}$ is constrained by a variety of factors (see Schouten et al.
455 (2013) and references therein), but the sources of isoGDGTs are considered to be
456 particularly important in continental archives. It is not suitable to apply calibrations of
457 $TEX_{86}$ in lacustrine environments if the lake sediments contained large amounts of
458 likely soil-derived isoGDGTs (Blaga et al., 2009, Powers et al., 2010), or if the lakes
459 have been strongly influenced by methanogenesis (Blaga et al., 2009). Here we tested
460 the applicability of $TEX_{86}$ to reconstruct lake water temperature in Chaka Salt Lake.

Interestingly, given the high allochthonous and methanogen inputs (see above), the reconstructed temperatures based on several lake calibrations (Powers et al., 2010, Tierney et al., 2010a, Castañeda and Schouten, 2011) are consistent with the measured surface water temperature of 17 °C (Fig. 6, and Table A2 in Supplementary material). The reconstructed summer lake surface temperature (Powers et al., 2010) is around 18 ± 10 °C, similar to the measured surface water temperature (Fig.6). Given the strong evidence that isoGDGTs derive from surrounding soils rather than the lake, we interpret the agreement between $TEX_{86}$-derived temperatures and lake temperatures as coincidental. Instead, this likely reflects the fact that $TEX_{86}$ values in soil can record soil temperatures (Yang et al., 2016). Indeed, using the relationship obtained for an altitudinal transect of Mt Xiangpi in China (Liu et al., 2013, Yang et al., 2016), our $TEX_{86}$ values yield MAT of -2 ± 3 °C, close to the observed MAAT of 5 °C.

*4.3.3. ACE*

The relative abundance of archaeol to GDGT-0, the ACE index (Equation 7), was originally proposed to track increasing salinity in marine and hypersaline environments (Turich and Freeman, 2011). ACE also appears to successfully document salinity change in northeastern Tibetan lakes and soils (Wang et al., 2013). However, Günther et al. (2014) showed that in southwestern Tibetan saline high mountain lakes, the relationship between the ACE index and salinity was complex (Günther et al., 2014).

Similarly, in tropical ponds, high ACE indices (between ca. 0.9 and 1) occur in ponds with markedly contrasting salinity, including low salinity, suggesting that it is not applicable to such settings (Huguet et al., 2015).

In our study, ACE indices of lake sediments (mean values 0.41) are higher than river sediments (mean value 0.09) and soils (mean value 0.03) (Table 1), as expected (although one river sediment RS4 has a higher ACE index of 0.18). However, the ACE indices of Chaka Salt Lake system are generally lower than those from marine environments (Turich and Freeman, 2011, Huguet et al., 2015), even though the water salinity of Chaka Salt Lake is ~10x higher. A high contribution of isoGDGTs, especially GDGT-0 from surrounding alkaline soils, as appears to be the case here, could bias the application of ACE index in lake sediments towards low values. This indicates that the sources of GDGT-0 in various saline environments should be constrained before the ACE index can be applied as a salinity proxy.

*4.3.4. MBT'/CBT*

In general, lake sediments from cold regions are dominated by brGDGT-III, whereas those from warmer regions are dominated by brGDGT-I (Tierney et al., 2010b, Loomis et al., 2011, Sun et al., 2011, Shanahan et al., 2013), in-line with the overall temperature dependence of brGDGTs with an increase in the degree of methylation at lower temperatures. Here, the relative abundance of GDGT-I was lower than GDGT-III in

501 both river and lake sediments (Fig. 3), in agreement with the low-temperature
502 continental climate of the region and mean annual water temperature of the lake of
503 5.0°C.

504 Temperatures derived from brGDGT distributions in soils range between -17.0 and
505 -11.3 °C (Table A2 in Supplementary material), when applying the original global soil
506 calibration (Weijers et al., 2007) and -5.7 to -2.3 °C with the revised calibration (Peterse
507 et al., 2012) (Fig. 7). Both are markedly lower than the instrumental MAAT of 5 °C and
508 lower than any modern soils in the calibration data set. In contrast to the global soil
509 calibrations, application of the regional soil calibration (Yang et al., 2014) yields
510 reconstructed temperatures more similar to the instrumental MAAT (Fig. 7). We
511 conclude that this better agreement is especially due to the fact that these regional soil
512 calibrations account for the impact of aridity on brGDGT distributions, which is known
513 to lead to an underestimation of MAAT (Peterse et al., 2012).

514 As discussed above (Sections 4.2 and 4.3.1), brGDGTs in river and lake sediments
515 appear not to derive from surrounding soils, but we cannot rule out the possibility of an
516 upland soil source. Therefore, we calculated MAAT of the sediments by using
517 soil-based calibrations (Fig. 7). Application of the original MBT-CBT calibration of
518 Weijers et al. (2007) to river and lake sediments yielded temperatures of 1.8 and -1.2 °C
519 respectively, slightly cooler than observed MAAT, taking into account the calibration
520 error (ca. 5 °C) (Fig. 7). Applying the revised MBT'-CBT calibration of Peterse et al.

(2012) to river and lake sediments yielded warmer reconstructed MAATs (5.9 and 4.1 °C) that were similar to observed MAAT.

In contrast, the regional soil calibration of Yang et al. (2014) resulted in relatively high MAATs ( 9.0 -10.4 °C), higher in fact by 3.8-5.4 °C than observed MAAT (Fig. 7). Therefore, among soil calibrations, it is the global calibration of Peterse et al. (2012) that is most consistent with MAATs in the Chaka Salt Lake catchment, even though soils of this area are not included in the global calibration. We suggest that this is because the regional Chinese calibration of Yang et al. (2014) is dominated by arid soils that are not representative of inputs to Chaka Salt Lake. Although the lake is surrounded by arid and alkaline soils, the brGDGTs in its sediments do not appear to derive from them, as discussed above. Instead, brGDGTs could derive from upland soils from less arid settings, such that a global calibration is more appropriate.

Alternatively, the brGDGTs could be produced *in situ* in lake sediments. To explore this, we applied various MAAT lake calibrations to the river and lake sediments (Fig. 8), but these all yielded temperature values (significantly) higher than observed MAAT. The best fit to a MAAT of 5 °C was obtained using the calibration of (Sun et al., 2011), which generated MAATs of 10.3 ± 1.1 °C and 8.2 ± 3.3 °C for river sediments and lake sediments, respectively. Therefore, unless a strong summer production bias is invoked, lake-based calibrations do not appear applicable to Chaka Salt Lake.

Therefore, the global soil calibrations appear to be most relevant Chaka Salt Lake –

541 although that also assumes an input from upland rather than local soils. Although that is
542 speculative, it is consistent with the lack of putative brGDGT-producing bacteria in the
543 lake. If so, it suggests that the MBT/CBT palaeothermometer can be used in hypersaline
544 systems, avoiding aridity biases that impact local soils, but it must be done so cautiously
545 given the complex controls on how such signals are carried through catchments.
546
547 **5. Conclusions**
548 We investigated the distributions of isoprenoid and branched GDGTs in river
549 sediments, lake sediments and soils from Chaka Salt Lake, an inland hypersaline lake in
550 China. Our work indicates that the GDGTs present in hypersaline lakes reflect both the
551 high salinity conditions of the lake but also the processes that govern GDGT
552 distributions and transport in the surrounding arid environment. We demonstrated that
553 methanogens likely had a significant contribution to the isoGDGT pool of the river and
554 lake sediments. Based on the low cren/cren' ratio in all samples, *Thaumarchaeota* group
555 I.1b likely were another major isoGDGT source, primarily from the surrounding
556 alkaline soils. This also appears to have biased the ACE Index, with high allochthonous
557 GDGT-0 inputs yielding lower-than-expected values. The brGDGT distributions in lake
558 and river sediments differed markedly from surrounding soils, and higher concentration
559 of brGDGTs occurred in lake sediments than soils, suggesting that at least part of the
560 brGDGTs were synthesized in either the lake or river. However, the contribution of

561 brGDGTs from upland soils cannot be excluded, and MAATs derived from lake
562 sediment brGDGTs appear to be consistent with such an origin.
563
564 **Acknowledgements**
565 We would like to thank F. Zheng, J. Xue, X. Qiu, H. Zhang, J. Lu and M. Huang for
566 sample collection and W. Ding for help with LC-MS maintenance. The work was
567 supported by the State Key R&D Program (grant No. 2016YFA0601104), Natural
568 Science Foundation of China (grants No. 41330103 and 41502173) and 111 Project
569 (grant No. B08030). We thank two anonymous reviewers for constructive and valuable
570 comments, which significantly improved the manuscript.
571

572

573 **References**

574 Bates, S.T., Berg-Lyons, D., Caporaso, J.G., Walters, W.A., Knight, R., Fierer, N., 2011.
575 Examining the global distribution of dominant archaeal populations in soil. The ISME
576 journal 5, 908-917.

577 Bechtel, A., Smittenberg, R.H., Bernasconi, S.M., Schubert, C.J., 2010. Distribution of
578 branched and isoprenoid tetraether lipids in an oligotrophic and a eutrophic Swiss lake:
579 insights into sources and GDGT-based proxies. Organic Geochemistry 41, 822-832.

580 Berke, M.A., Johnson, T.C., Werne, J.P., Grice, K., Schouten, S., Sinninghe Damsté,
581 J.S., 2012. Molecular records of climate variability and vegetation response since the
582 Late Pleistocene in the Lake Victoria basin, East Africa. Quaternary Science Reviews
583 55, 59-74.

584 Birgel, D., Guido, A., Liu, X., Hinrichs, K.-U., Gier, S., Peckmann, J., 2014.
585 Hypersaline conditions during deposition of the Calcare di Base revealed from archaeal
586 di- and tetraether inventories. Organic Geochemistry 77, 11-21.

587 Blaga, C.I., Reichart, G.-J., Heiri, O., Damsté, J.S.S., 2009. Tetraether membrane lipid
588 distributions in water-column particulate matter and sediments: a study of 47 European
589 lakes along a north–south transect. Journal of Paleolimnology 41, 523-540.

590 Blaga, C.I., Reichart, G.-J., Schouten, S., Lotter, A.F., Werne, J.P., Kosten, S., Mazzeo,

591 N., Lacerot, G., Damsté, J.S.S., 2010. Branched glycerol dialkyl glycerol tetraethers in
592 lake sediments: Can they be used as temperature and pH proxies? Organic
593 Geochemistry 41, 1225-1234.

594 Blaga, C.I., Reichart, G.-J., Lotter, A.F., Anselmetti, F.S., Sinninghe Damsté, J.S., 2013.
595 A TEX86 lake record suggests simultaneous shifts in temperature in Central Europe and
596 Greenland during the last deglaciation. Geophysical Research Letters 40, 948-953.

597 Castañeda, I.S., Schouten, S., 2011. A review of molecular organic proxies for
598 examining modern and ancient lacustrine environments. Quaternary Science Reviews
599 30, 2851-2891.

600 D'Anjou, R., Wei, J., Castaneda, I., Brigham-Grette, J., Petsch, S., Finkelstein, D., 2013.
601 High-latitude environmental change during MIS 9 and 11: biogeochemical evidence
602 from Lake El'gygytgyn, Far East Russia. Climate of the Past 9, 567-581.

603 Das, S.K., Bendle, J., Routh, J., 2012. Evaluating branched tetraether lipid-based
604 palaeotemperature proxies in an urban, hyper-eutrophic polluted lake in South Africa.
605 Organic Geochemistry 53, 45-51.

606 De Jonge, C., Hopmans, E.C., Stadnitskaia, A., Rijpstra, W.I.C., Hofland, R., Tegelaar,
607 E., Damsté, J.S.S., 2013. Identification of novel penta-and hexamethylated branched
608 glycerol dialkyl glycerol tetraethers in peat using HPLC–MS 2, GC–MS and GC–
609 SMB-MS. Organic Geochemistry 54, 78-82.

610 De Jonge, C., Hopmans, E.C., Zell, C.I., Kim, J.-H., Schouten, S., Damsté, J.S.S., 2014a.
611 Occurrence and abundance of 6-methyl branched glycerol dialkyl glycerol tetraethers in
612 soils: Implications for palaeoclimate reconstruction. Geochimica et Cosmochimica Acta
613 141, 97-112.

614 De Jonge, C., Stadnitskaia, A., Hopmans, E.C., Cherkashov, G., Fedotov, A., Damsté,
615 J.S.S., 2014b. In situ produced branched glycerol dialkyl glycerol tetraethers in
616 suspended particulate matter from the Yenisei River, Eastern Siberia. Geochimica et
617 Cosmochimica Acta 125, 476-491.

618 De La Torre, J.R., Walker, C.B., Ingalls, A.E., Könneke, M., Stahl, D.A., 2008.
619 Cultivation of a thermophilic ammonia oxidizing archaeon synthesizing crenarchaeol.
620 Environmental Microbiology 10, 810-818.

621 Dirghangi, S.S., Pagani, M., Hren, M.T., Tipple, B.J., 2013. Distribution of glycerol
622 dialkyl glycerol tetraethers in soils from two environmental transects in the USA.
623 Organic Geochemistry 59, 49-60.

624 Duan, Y., Zhao, Y., Sun, T., Zhang, X., 2014. δD values of individual n-alkanes in
625 sediments from the Chaka salt lake (China) and terrestrial plants from the surrounding
626 area. Geochemical Journal 48, 321-329.

627 Günther, F., Thiele, A., Gleixner, G., Xu, B., Yao, T., Schouten, S., 2014. Distribution
628 of bacterial and archaeal ether lipids in soils and surface sediments of Tibetan lakes:

629 implications for GDGT-based proxies in saline high mountain lakes. Organic
630 Geochemistry 67, 19-30.

631 Hopmans, E.C., Weijers, J.W.H., Schefuß, E., Herfort, L., Sinninghe Damsté, J.S.,
632 Schouten, S., 2004. A novel proxy for terrestrial organic matter in sediments based on
633 branched and isoprenoid tetraether lipids. Earth and Planetary Science Letters 224,
634 107-116.

635 Huguet, A., Grossi, V., Belmahdi, I., Fosse, C., Derenne, S., 2015. Archaeal and
636 bacterial tetraether lipids in tropical ponds with contrasting salinity (Guadeloupe,
637 French West Indies): Implications for tetraether-based environmental proxies. Organic
638 Geochemistry 83–84, 158-169.

639 Huguet, C., Hopmans, E.C., Febo-Ayala, W., Thompson, D.H., Sinninghe Damsté, J.S.,
640 Schouten, S., 2006. An improved method to determine the absolute abundance of
641 glycerol dibiphytanyl glycerol tetraether lipids. Organic Geochemistry 37, 1036-1041.

642 Jiang, H., Dong, H., Zhang, G., Yu, B., Chapman, L.R., Fields, M.W., 2006. Microbial
643 diversity in water and sediment of Lake Chaka, an athalassohaline lake in northwestern
644 China. Applied and environmental microbiology 72, 3832-3845.

645 Jiang, H., Dong, H., Yu, B., Liu, X., Li, Y., Ji, S., Zhang, C.L., 2007. Microbial
646 response to salinity change in Lake Chaka, a hypersaline lake on Tibetan plateau.
647 Environmental Microbiology 9, 2603-2621.

Jung, M.-Y., Park, S.-J., Min, D., Kim, J.-S., Rijpstra, W.I.C., Sinninghe Damsté, J.S., Kim, G.-J., Madsen, E.L., Rhee, S.-K., 2011. Enrichment and Characterization of an Autotrophic Ammonia-Oxidizing Archaeon of Mesophilic Crenarchaeal Group I.1a from an Agricultural Soil. Applied and Environmental Microbiology 77, 8635-8647.

Karner, M.B., DeLong, E.F., Karl, D.M., 2001. Archaeal dominance in the mesopelagic zone of the Pacific Ocean. Nature 409, 507-510.

Keough, B., Schmidt, T., Hicks, R., 2003. Archaeal nucleic acids in picoplankton from great lakes on three continents. Microbial Ecology 46, 238-248.

Kim, J.-G., Jung, M.-Y., Park, S.-J., Rijpstra, W.I.C., Sinninghe Damsté, J.S., Madsen, E.L., Min, D., Kim, J.-S., Kim, G.-J., Rhee, S.-K., 2012. Cultivation of a highly enriched ammonia-oxidizing archaeon of thaumarchaeotal group I.1b from an agricultural soil. Environmental Microbiology 14, 1528-1543.

Kim, J.-H., Van der Meer, J., Schouten, S., Helmke, P., Willmott, V., Sangiorgi, F., Koç, N., Hopmans, E.C., Damsté, J.S.S., 2010. New indices and calibrations derived from the distribution of crenarchaeal isoprenoid tetraether lipids: Implications for past sea surface temperature reconstructions. Geochimica et Cosmochimica Acta 74, 4639-4654.

Lehtovirta-Morley, L.E., Stoecker, K., Vilcinskas, A., Prosser, J.I., Nicol, G.W., 2011. Cultivation of an obligate acidophilic ammonia oxidizer from a nitrifying acid soil. Proceedings of the National Academy of Sciences 108, 15892-15897.

667 Lincoln, S.A., Wai, B., Eppley, J.M., Church, M.J., Summons, R.E., DeLong, E.F.,
668 2014a. Planktonic Euryarchaeota are a significant source of archaeal tetraether lipids in
669 the ocean. Proceedings of the National Academy of Sciences 111, 9858-9863.

670 Lincoln, S.A., Wai, B., Eppley, J.M., Church, M.J., Summons, R.E., DeLong, E.F.,
671 2014b. Reply to Schouten et al.: Marine Group II planktonic Euryarchaeota are
672 significant contributors to tetraether lipids in the ocean. Proceedings of the National
673 Academy of Sciences of the United States of America 111, E4286.

674 Liu, W., Wang, H., Zhang, C.L., Liu, Z., He, Y., 2013. Distribution of glycerol dialkyl
675 glycerol tetraether lipids along an altitudinal transect on Mt. Xiangpi, NE
676 Qinghai-Tibetan Plateau, China. Organic Geochemistry 57, 76-83.

677 Liu, X., Dong, H., Rech, J.A., Ryo, M., Yang, B., Wang, Y., 2008. Evolution of Chaka
678 Salt Lake in NW China in response to climatic change during the Latest Pleistocene–
679 Holocene. Quaternary Science Reviews 27, 867-879.

680 Loomis, S.E., Russell, J.M., Damsté, J.S.S., 2011. Distributions of branched GDGTs in
681 soils and lake sediments from western Uganda: implications for a lacustrine
682 paleothermometer. Organic Geochemistry 42, 739-751.

683 Loomis, S.E., Russell, J.M., Ladd, B., Street-Perrott, F.A., Sinninghe Damsté, J.S., 2012.
684 Calibration and application of the branched GDGT temperature proxy on East African
685 lake sediments. Earth and Planetary Science Letters 357–358, 277-288.

686 Loomis, S.E., Russell, J.M., Heureux, A.M., D'Andrea, W.J., Sinninghe Damsté, J.S.,
687 2014. Seasonal variability of branched glycerol dialkyl glycerol tetraethers (brGDGTs)
688 in a temperate lake system. Geochimica et Cosmochimica Acta 144, 173-187.

689 Naeher, S., Smittenberg, R.H., Gilli, A., Kirilova, E.P., Lotter, A.F., Schubert, C.J.,
690 2012. Impact of recent lake eutrophication on microbial community changes as revealed
691 by high resolution lipid biomarkers in Rotsee (Switzerland). Organic Geochemistry 49,
692 86-95.

693 Naeher, S., Peterse, F., Smittenberg, R.H., Niemann, H., Zigah, P.K., Schubert, C.J.,
694 2014. Sources of glycerol dialkyl glycerol tetraethers (GDGTs) in catchment soils,
695 water column and sediments of Lake Rotsee (Switzerland) – Implications for the
696 application of GDGT-based proxies for lakes. Organic Geochemistry 66, 164-173.

697 Niemann, H., Stadnitskaia, A., Wirth, S., Gilli, A., Anselmetti, F., Sinninghe Damsté, J.,
698 Schouten, S., Hopmans, E., Lehmann, M., 2012. Bacterial GDGTs in Holocene
699 sediments and catchment soils of a high Alpine lake: application of the
700 MBT/CBT-paleothermometer. Climate of the Past 8, 889-906.

701 Pancost, R., Hopmans, E., Sinninghe Damste, J., Woodside, J., 2001. Archaeal lipids in
702 Mediterranean cold seeps: molecular proxies for anaerobic methane oxidation.

703 Pearson, A., Ingalls, A.E., 2013. Assessing the use of archaeal lipids as marine
704 environmental proxies. Annual Review of Earth and Planetary Sciences 41, 359-384.

705 Pearson, E.J., Juggins, S., Talbot, H.M., Weckström, J., Rosén, P., Ryves, D.B., Roberts,
706 S.J., Schmidt, R., 2011. A lacustrine GDGT-temperature calibration from the
707 Scandinavian Arctic to Antarctic: renewed potential for the application of
708 GDGT-paleothermometry in lakes. Geochimica et Cosmochimica Acta 75, 6225-6238.

709 Peterse, F., Kim, J.-H., Schouten, S., Kristensen, D.K., Koç, N., Sinninghe Damsté, J.S.,
710 2009. Constraints on the application of the MBT/CBT palaeothermometer at high
711 latitude environments (Svalbard, Norway). Organic Geochemistry 40, 692-699.

712 Peterse, F., Nicol, G.W., Schouten, S., Sinninghe Damsté, J.S., 2010. Influence of soil
713 pH on the abundance and distribution of core and intact polar lipid-derived branched
714 GDGTs in soil. Organic Geochemistry 41, 1171-1175.

715 Peterse, F., van der Meer, J., Schouten, S., Weijers, J.W., Fierer, N., Jackson, R.B., Kim,
716 J.-H., Damsté, J.S.S., 2012. Revised calibration of the MBT–CBT paleotemperature
717 proxy based on branched tetraether membrane lipids in surface soils. Geochimica et
718 Cosmochimica Acta 96, 215-229.

719 Peterse, F., Vonk, J.E., Holmes, R.M., Giosan, L., Zimov, N., Eglinton, T.I., 2014.
720 Branched glycerol dialkyl glycerol tetraethers in Arctic lake sediments: Sources and
721 implications for paleothermometry at high latitudes. Journal of Geophysical Research:
722 Biogeosciences 119, 2014JG002639.

723 Pitcher, A., Rychlik, N., Hopmans, E.C., Spieck, E., Rijpstra, W.I.C., Ossebaar, J.,

724 Schouten, S., Wagner, M., Damsté, J.S.S., 2010. Crenarchaeol dominates the membrane
725 lipids of Candidatus Nitrososphaera gargensis, a thermophilic Group I. 1b Archaeon.
726 The ISME journal 4, 542-552.

727 Powers, L., Werne, J.P., Vanderwoude, A.J., Damsté, J.S.S., Hopmans, E.C., Schouten,
728 S., 2010. Applicability and calibration of the TEX 86 paleothermometer in lakes.
729 Organic Geochemistry 41, 404-413.

730 Schoon, P.L., de Kluijver, A., Middelburg, J.J., Downing, J.A., Sinninghe Damsté, J.S.,
731 Schouten, S., 2013. Influence of lake water pH and alkalinity on the distribution of core
732 and intact polar branched glycerol dialkyl glycerol tetraethers (GDGTs) in lakes.
733 Organic Geochemistry 60, 72-82.

734 Schouten, S., Hopmans, E.C., Schefuß, E., Sinninghe Damsté, J.S., 2002. Distributional
735 variations in marine crenarchaeotal membrane lipids: a new tool for reconstructing
736 ancient sea water temperatures? Earth and Planetary Science Letters 204, 265-274.

737 Schouten, S., Hopmans, E.C., Sinninghe Damsté, J.S., 2013. The organic geochemistry
738 of glycerol dialkyl glycerol tetraether lipids: A review. Organic Geochemistry 54,
739 19-61.

740 Schouten, S., Villanueva, L., Hopmans, E.C., van der Meer, M.T., Damsté, J.S.S., 2014.
741 Are Marine Group II Euryarchaeota significant contributors to tetraether lipids in the
742 ocean? Proceedings of the National Academy of Sciences of the United States of

743 America 111, E4285.

744 Shanahan, T.M., Hughen, K.A., Van Mooy, B.A.S., 2013. Temperature sensitivity of
745 branched and isoprenoid GDGTs in Arctic lakes. Organic Geochemistry 64, 119-128.

746 Sinninghe Damsté, J.S., Hopmans, E.C., Pancost, R.D., Schouten, S., Geenevasen, J.A.,
747 2000. Newly discovered non-isoprenoid glycerol dialkyl glycerol tetraether lipids in
748 sediments. Chemical Communications, 1683-1684.

749 Sinninghe Damsté, J.S., Rijpstra, W.I.C., Hopmans, E.C., Prahl, F.G., Wakeham, S.G.,
750 Schouten, S., 2002. Distribution of Membrane Lipids of Planktonic Crenarchaeota in
751 the Arabian Sea. Applied and Environmental Microbiology 68, 2997-3002.

752 Sinninghe Damsté, J.S., Ossebaar, J., Abbas, B., Schouten, S., Verschuren, D., 2009.
753 Fluxes and distribution of tetraether lipids in an equatorial African lake: constraints on
754 the application of the TEX 86 palaeothermometer and BIT index in lacustrine settings.
755 Geochimica et Cosmochimica Acta 73, 4232-4249.

756 Sinninghe Damsté, J.S., Rijpstra, W.I.C., Hopmans, E.C., Weijers, J.W.H., Foesel, B.U.,
757 Overmann, J., Dedysh, S.N., 2011. 13,16-Dimethyl Octacosanedioic Acid (iso-Diabolic
758 Acid), a Common Membrane-Spanning Lipid of Acidobacteria Subdivisions 1 and 3.
759 Applied and Environmental Microbiology 77, 4147-4154.

760 Sinninghe Damsté, J.S., Ossebaar, J., Schouten, S., Verschuren, D., 2012a. Distribution

761 of tetraether lipids in the 25-ka sedimentary record of Lake Challa: extracting reliable
762 TEX86 and MBT/CBT palaeotemperatures from an equatorial African lake. Quaternary
763 Science Reviews 50, 43-54.

764 Sinninghe Damsté, J.S., Rijpstra, W.I.C., Hopmans, E.C., Jung, M.-Y., Kim, J.-G., Rhee,
765 S.-K., Stieglmeier, M., Schleper, C., 2012b. Intact Polar and Core Glycerol
766 Dibiphytanyl Glycerol Tetraether Lipids of Group I.1a and I.1b Thaumarchaeota in Soil.
767 Applied and Environmental Microbiology 78, 6866-6874.

768 Sinninghe Damsté, J.S., Rijpstra, W.I.C., Hopmans, E.C., Foesel, B.U., Wüst, P.K.,
769 Overmann, J., Tank, M., Bryant, D.A., Dunfield, P.F., Houghton, K., Stott, M.B., 2014.
770 Ether- and Ester-Bound iso-Diabolic Acid and Other Lipids in Members of
771 Acidobacteria Subdivision 4. Applied and Environmental Microbiology 80, 5207-5218.

772 Sun, Q., Chu, G., Liu, M., Xie, M., Li, S., Ling, Y., Wang, X., Shi, L., Jia, G., Lü, H.,
773 2011. Distributions and temperature dependence of branched glycerol dialkyl glycerol
774 tetraethers in recent lacustrine sediments from China and Nepal. Journal of Geophysical
775 Research: Biogeosciences (2005–2012) 116.

776 Tierney, J.E., Russell, J.M., Huang, Y., Damsté, J.S.S., Hopmans, E.C., Cohen, A.S.,
777 2008. Northern hemisphere controls on tropical southeast African climate during the
778 past 60,000 years. Science 322, 252-255.

779 Tierney, J.E., Russell, J.M., 2009. Distributions of branched GDGTs in a tropical lake

780 system: Implications for lacustrine application of the MBT/CBT paleoproxy. Organic
781 Geochemistry 40, 1032-1036.

782 Tierney, J.E., Mayes, M.T., Meyer, N., Johnson, C., Swarzenski, P.W., Cohen, A.S.,
783 Russell, J.M., 2010a. Late-twentieth-century warming in Lake Tanganyika
784 unprecedented since AD 500. Nature Geoscience 3, 422-425.

785 Tierney, J.E., Russell, J.M., Eggermont, H., Hopmans, E., Verschuren, D., Damsté, J.S.,
786 2010b. Environmental controls on branched tetraether lipid distributions in tropical East
787 African lake sediments. Geochimica et Cosmochimica Acta 74, 4902-4918.

788 Turich, C., Freeman, K.H., 2011. Archaeal lipids record paleosalinity in hypersaline
789 systems. Organic Geochemistry 42, 1147-1157.

790 Tyler, J.J., Nederbragt, A.J., Jones, V.J., Thurow, J.W., 2010. Assessing past
791 temperature and soil pH estimates from bacterial tetraether membrane lipids: Evidence
792 from the recent lake sediments of Lochnagar, Scotland. Journal of Geophysical
793 Research: Biogeosciences 115, G01015.

794 Wang, H., Liu, W., Zhang, C.L., Wang, Z., Wang, J., Liu, Z., Dong, H., 2012.
795 Distribution of glycerol dialkyl glycerol tetraethers in surface sediments of Lake
796 Qinghai and surrounding soil. Organic Geochemistry 47, 78-87.

797 Wang, H., Liu, W., Zhang, C.L., Jiang, H., Dong, H., Lu, H., Wang, J., 2013. Assessing

798 the ratio of archaeol to caldarchaeol as a salinity proxy in highland lakes on the
799 northeastern Qinghai–Tibetan Plateau. Organic Geochemistry 54, 69-77.

800 Weijers, J.W.H., Schouten, S., Hopmans, E.C., Geenevasen, J.A.J., David, O.R.P.,
801 Coleman, J.M., Pancost, R.D., Sinninghe Damsté, J.S., 2006. Membrane lipids of
802 mesophilic anaerobic bacteria thriving in peats have typical archaeal traits.
803 Environmental Microbiology 8, 648-657.

804 Weijers, J.W.H., Schouten, S., van den Donker, J.C., Hopmans, E.C., Sinninghe Damsté,
805 J.S., 2007. Environmental controls on bacterial tetraether membrane lipid distribution in
806 soils. Geochimica et Cosmochimica Acta 71, 703-713.

807 Woltering, M., Johnson, T.C., Werne, J.P., Schouten, S., Damsté, J.S.S., 2011. Late
808 Pleistocene temperature history of Southeast Africa: a TEX 86 temperature record from
809 Lake Malawi. Palaeogeography, Palaeoclimatology, Palaeoecology 303, 93-102.

810 Xie, S., Pancost, R.D., Chen, L., Evershed, R.P., Yang, H., Zhang, K., Huang, J., Xu, Y.,
811 2012. Microbial lipid records of highly alkaline deposits and enhanced aridity
812 associated with significant uplift of the Tibetan Plateau in the Late Miocene. Geology
813 40, 291-294.

814 Yang, H., Ding, W., Wang, J., Jin, C., He, G., Qin, Y., Xie, S., 2012. Soil pH impact on
815 microbial tetraether lipids and terrestrial input index (BIT) in China. Science China
816 Earth Sciences 55, 236-245.

817 Yang, H., Pancost, R.D., Dang, X., Zhou, X., Evershed, R.P., Xiao, G., Tang, C., Gao,
818 L., Guo, Z., Xie, S., 2014. Correlations between microbial tetraether lipids and
819 environmental variables in Chinese soils: Optimizing the paleo-reconstructions in
820 semi-arid and arid regions. Geochimica et Cosmochimica Acta 126, 49-69.

821 Yang, H., Pancost, R.D., Jia, C., Xie, S., 2016. The Response of Archaeal Tetraether
822 Membrane Lipids in Surface Soils to Temperature: A Potential Paleothermometer in
823 Paleosols. Geomicrobiology Journal 33, 98-109.

824 Yang, J., Jiang, H., Dong, H., Wang, H., Wu, G., Hou, W., Liu, W., Zhang, C., Sun, Y.,
825 Lai, Z., 2013. amoA-encoding archaea and thaumarchaeol in the lakes on the
826 northeastern Qinghai-Tibetan Plateau, China. Frontiers in microbiology 4.

827 Zell, C., Kim, J.-H., Moreira-Turcq, P., Abril, G., Hopmans, E.C., Bonnet, M.-P.,
828 Sobrinho, R.L., Damsté, J.S.S., 2013. Disentangling the origins of branched tetraether
829 lipids and crenarchaeol in the lower Amazon River: Implications for GDGT‐based
830 proxies. Limnology and Oceanography 58, 343-353.

831 Zheng, X., Zhang, M., Li, B., Xu, C., 2002. Salt lakes of China. Beijing: Science Press.
832

833

834 **Tables**

835 **Table 1**

836 Fractional abundance of isoGDGTs and isoGDGT-based proxies for river sediments

837 (RS), lake sediments (LS) and soils (S) in and around Chaka Salt Lake

| Sample | Lat.( N) | Long.( E) | Fractional abundance of isoGDGTs (%) | | | | | | Total isoGDGTs (μg/g TOC) | TOC(%) | BIT | $R_{I/b}$ | $TEX_{86}$ | cren/cren' | GDGT-0/cren | ACE |
|---|---|---|---|---|---|---|---|---|---|---|---|---|---|---|---|---|
| | | | GDGT-0 | GDGT-1 | GDGT-2 | GDGT-3 | cren | cren' | | | | | | | | |
| RS1 | 36°47.496′ | 99°01.296′ | 55.8 | 5.3 | 7.4 | 3.4 | 25.9 | 2.2 | 1.09 | 1.84 | 0.69 | 1.28 | 0.71 | 11.84 | 2.16 | 0.11 |
| RS2 | 36°47.368′ | 99°01.293′ | 78.9 | 3.7 | 4.0 | 1.4 | 11.1 | 0.9 | 2.04 | 1.34 | 0.91 | 0.63 | 0.63 | 13.00 | 7.10 | 0.01 |
| RS3 | 36°47.219′ | 99°01.304′ | 66.4 | 5.0 | 6.3 | 2.7 | 18.1 | 1.5 | 0.58 | 1.58 | 0.80 | 0.89 | 0.68 | 12.21 | 3.66 | 0.07 |
| RS4 | 36°46.801′ | 99°01.329′ | 49.5 | 6.9 | 9.2 | 3.6 | 29.0 | 1.8 | 1.11 | 0.83 | 0.69 | 0.98 | 0.68 | 16.21 | 1.71 | 0.18 |
| LS5 | 36°44.719′ | 99°03.379′ | 71.6 | 19.5 | 6.1 | 1.2 | 1.4 | 0.1 | 2.56 | 1.71 | 0.81 | 14.35 | 0.28 | 11.13 | 52.41 | 0.16 |
| LS6 | 36°44.913′ | 99°02.839′ | 54.9 | 5.8 | 8.2 | 3.9 | 25.2 | 1.9 | 1.60 | 0.97 | 0.76 | 0.92 | 0.71 | 13.06 | 2.18 | 0.43 |
| LS7 | 36°44.768′ | 99°02.896′ | 45.2 | 6.4 | 9.7 | 4.3 | 31.8 | 2.6 | 0.52 | 2.03 | 0.56 | 1.81 | 0.72 | 12.24 | 1.42 | 0.66 |
| LS8 | 36°44.366′ | 99°02.752′ | 74.2 | 17.2 | 5.2 | 1.2 | 2.0 | 0.2 | 0.99 | 1.60 | 0.81 | 10.02 | 0.28 | 10.91 | 38.00 | 0.16 |
| LS9 | 36°44.309′ | 99°02.765′ | 69.6 | 16.9 | 6.7 | 2.0 | 4.3 | 0.5 | 0.51 | 1.39 | 0.79 | 4.99 | 0.35 | 8.51 | 16.33 | 0.43 |
| LS10 | 36°44.526′ | 99°02.704′ | 28.2 | 12.2 | 12.5 | 8.5 | 32.6 | 6.0 | 0.06 | 2.67 | 0.36 | 2.43 | 0.69 | 5.47 | 0.86 | 0.63 |
| S11 | 36°43.509′ | 98°52.185′ | 25.6 | 7.8 | 12.6 | 4.4 | 47.6 | 2.0 | 1.05 | 0.79 | 0.52 | 1.79 | 0.71 | 23.51 | 0.54 | 0.01 |
| S12 | 36°43.525′ | 98°52.157′ | 21.4 | 8.0 | 15.6 | 5.8 | 45.0 | 4.2 | 0.82 | 0.81 | 0.70 | 0.90 | 0.76 | 10.74 | 0.48 | 0.14 |
| S13 | 36°43.352′ | 98°52.245′ | 52.7 | 5.4 | 6.4 | 2.4 | 31.8 | 1.4 | 0.68 | 0.86 | 0.53 | 2.65 | 0.65 | 23.03 | 1.66 | 0.01 |
| S14 | 36°40.906′ | 98°52.673′ | 33.7 | 7.8 | 9.4 | 3.4 | 44.3 | 1.5 | 0.51 | 2.26 | 0.49 | 2.28 | 0.65 | 29.86 | 0.76 | 0.00 |
| S15 | 36°41.176′ | 98°53.049′ | 79.8 | 2.7 | 3.4 | 1.4 | 12.1 | 0.6 | 0.08 | 1.30 | 0.62 | 4.80 | 0.66 | 21.66 | 6.60 | 0.01 |

838

**Table 2**

Fractional abundance of brGDGTs and brGDGT-based proxies for river sediments (RS), lake sediments (LS) and soils (S) in and around Chaka Salt Lake

| Sample | Lat.( N) | Long.( E) | Fractional abundance of brGDGTs (%) | | | | | | | | | Total brGDGTs (μg/g TOC) | TOC(%) | MBT | CBT | MBT' |
|---|---|---|---|---|---|---|---|---|---|---|---|---|---|---|---|---|
| | | | III | IIIb | IIIc | II | IIb | IIc | I | Ib | Ic | | | | | |
| RS1 | 36°47.496′ | 99°01.296′ | 33.6 | 1.9 | 0.2 | 29.3 | 13.4 | 1.6 | 9.6 | 5.4 | 5.0 | 0.85 | 1.84 | 0.20 | 0.31 | 0.20 |
| RS2 | 36°47.368′ | 99°01.293′ | 30.3 | 1.9 | 0.3 | 35.0 | 15.2 | 0.9 | 7.7 | 7.9 | 0.9 | 3.27 | 1.34 | 0.17 | 0.27 | 0.17 |
| RS3 | 36°47.219′ | 99°01.304′ | 28.8 | 3.0 | 0.5 | 27.6 | 16.0 | 2.4 | 8.6 | 9.1 | 4.0 | 0.64 | 1.58 | 0.22 | 0.16 | 0.23 |
| RS4 | 36°46.801′ | 99°01.329′ | 27.5 | 3.4 | 0.6 | 26.8 | 18.9 | 2.7 | 8.4 | 8.0 | 3.8 | 1.13 | 0.83 | 0.20 | 0.12 | 0.21 |
| LS5 | 36°44.719′ | 99°03.379′ | 50.0 | 2.9 | 0.3 | 27.0 | 7.5 | 0.8 | 9.1 | 1.8 | 0.7 | 0.18 | 1.71 | 0.12 | 0.59 | 0.12 |
| LS6 | 36°44.913′ | 99°02.839′ | 30.8 | 3.3 | 0.6 | 32.5 | 16.9 | 1.6 | 8.3 | 4.9 | 0.9 | 1.74 | 0.97 | 0.14 | 0.27 | 0.15 |
| LS7 | 36°44.768′ | 99°02.896′ | 34.0 | 2.9 | 0.4 | 31.9 | 15.4 | 1.3 | 7.7 | 5.1 | 1.3 | 0.29 | 2.03 | 0.14 | 0.29 | 0.15 |
| LS8 | 36°44.366′ | 99°02.752′ | 48.5 | 3.5 | 0.9 | 24.8 | 7.3 | 1.1 | 8.9 | 3.3 | 1.8 | 0.10 | 1.60 | 0.14 | 0.50 | 0.15 |
| LS9 | 36°44.309′ | 99°02.765′ | 45.4 | 2.4 | 0.0 | 25.7 | 10.6 | 2.5 | 6.7 | 3.9 | 2.7 | 0.10 | 1.39 | 0.13 | 0.35 | 0.14 |
| LS10 | 36°44.526′ | 99°02.704′ | 12.6 | 2.5 | 0.0 | 25.2 | 25.5 | 6.8 | 6.3 | 11.4 | 9.7 | 0.03 | 2.67 | 0.27 | -0.07 | 0.28 |
| S11 | 36°43.509′ | 98°52.185′ | 50.6 | 1.2 | 0.1 | 37.6 | 1.5 | 1.8 | 5.0 | 0.5 | 1.6 | 0.59 | 0.79 | 0.07 | 1.33 | 0.07 |
| S12 | 36°43.525′ | 98°52.157′ | 53.0 | 1.4 | 0.2 | 36.5 | 2.4 | 0.5 | 4.8 | 0.5 | 0.5 | 0.91 | 0.81 | 0.06 | 1.14 | 0.06 |
| S13 | 36°43.352′ | 98°52.245′ | 45.0 | 0.8 | 0.3 | 45.4 | 1.6 | 0.7 | 5.6 | 0.6 | 0.0 | 0.26 | 0.86 | 0.06 | 1.38 | 0.06 |
| S14 | 36°40.906′ | 98°52.673′ | 53.8 | 0.5 | 0.0 | 37.0 | 1.1 | 1.7 | 4.5 | 0.3 | 1.2 | 0.22 | 2.26 | 0.06 | 1.47 | 0.06 |
| S15 | 36°41.176′ | 98°53.049′ | 45.9 | 0.0 | 0.0 | 39.8 | 4.9 | 1.8 | 7.5 | 0.0 | 0.0 | 0.02 | 1.30 | 0.08 | 0.98 | 0.08 |

843

844 Figure Captions

845 **Fig.1.** Chemical structures and molecular ion *m/z* values for glycerol dialkyl glycerol
846 tetraethers (GDGTs) and archaeol.

847 **Fig.2**. Map of Chaka Salt Lake showing locations of samples. Sampling sites
848 correspond to Table 1 and Table 2.

849 **Fig.3.** Fractional abundance of GDGT 0-3, crenarchaeol, crenarchaeol' and GDGT I-III
850 as fractions of the sum of all GDGTs in river sediments, lake sediments and soils.

851 **Fig.4.** Box plot showing scale values of cren/cren' in soil, lake sediments and marine
852 sediments, as well as Thaumarchaeota Group I.1a and Group I.1b from published
853 literature (De La Torre et al., 2008, Blaga et al., 2009, Kim et al., 2010, Jung et al., 2011,
854 Lehtovirta-Morley et al., 2011, Kim et al., 2012, Sinninghe Damsté et al., 2012b, Wang
855 et al., 2012, Yang et al., 2012).

856 **Fig.5.** Plots showing the distributions of MBT and CBT indices in river sediments, lake
857 sediments and soils.

858 **Fig.6.** Comparison of reconstructed temperature based on lake $TEX_{86}$ calibrations in
859 lake sediments as listed from Eq. 8 to Eq. 12.

860 **Fig.7.** Comparison of reconstructed temperature based on soil calibrations in soils, river
861 sediments and lake sediments as listed from Eq. 13 to Eq. 16.

862 **Fig.8.** Comparison of reconstructed temperature based on lake calibrations as listed

from Eq. 17 to Eq. 23. Calibrations of MBT/CBT and fractional abundance of branched GDGTs were applied to river sediments and lake sediments.

866

867 Figure 1

868

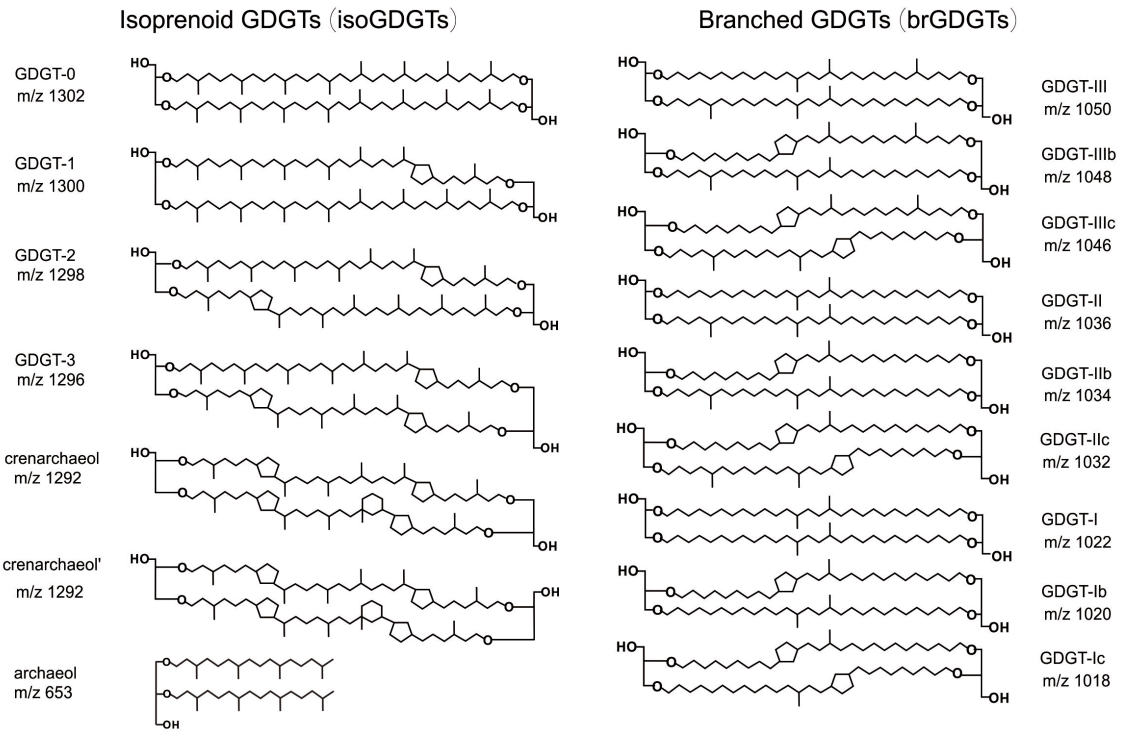


869

870 Figure 2

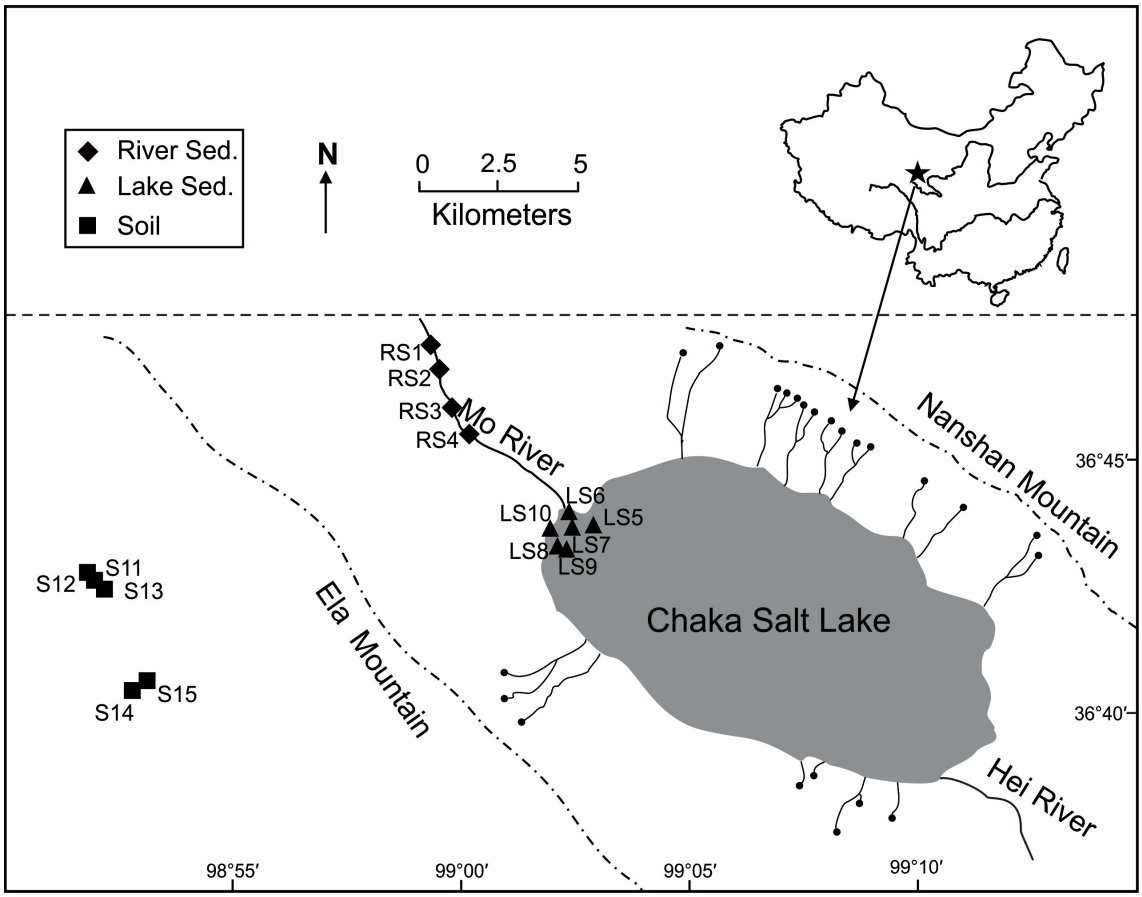


871

872 Figure 3

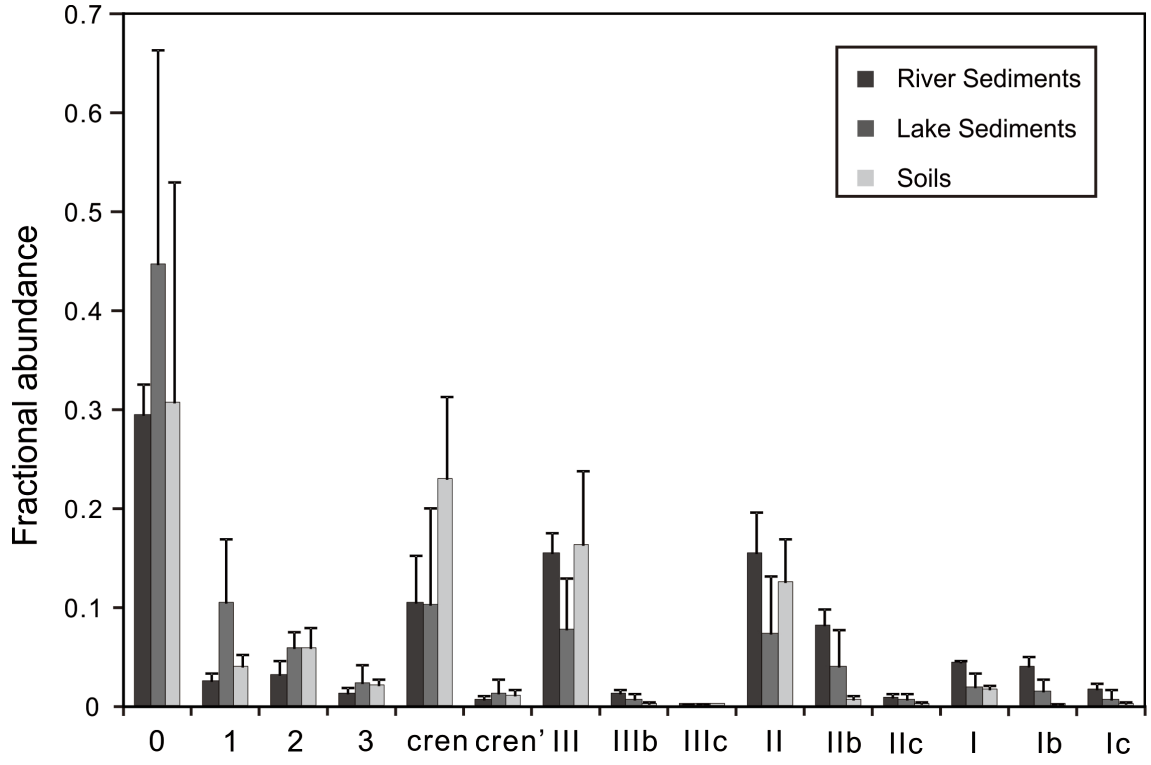


873

874

875 Figure 4

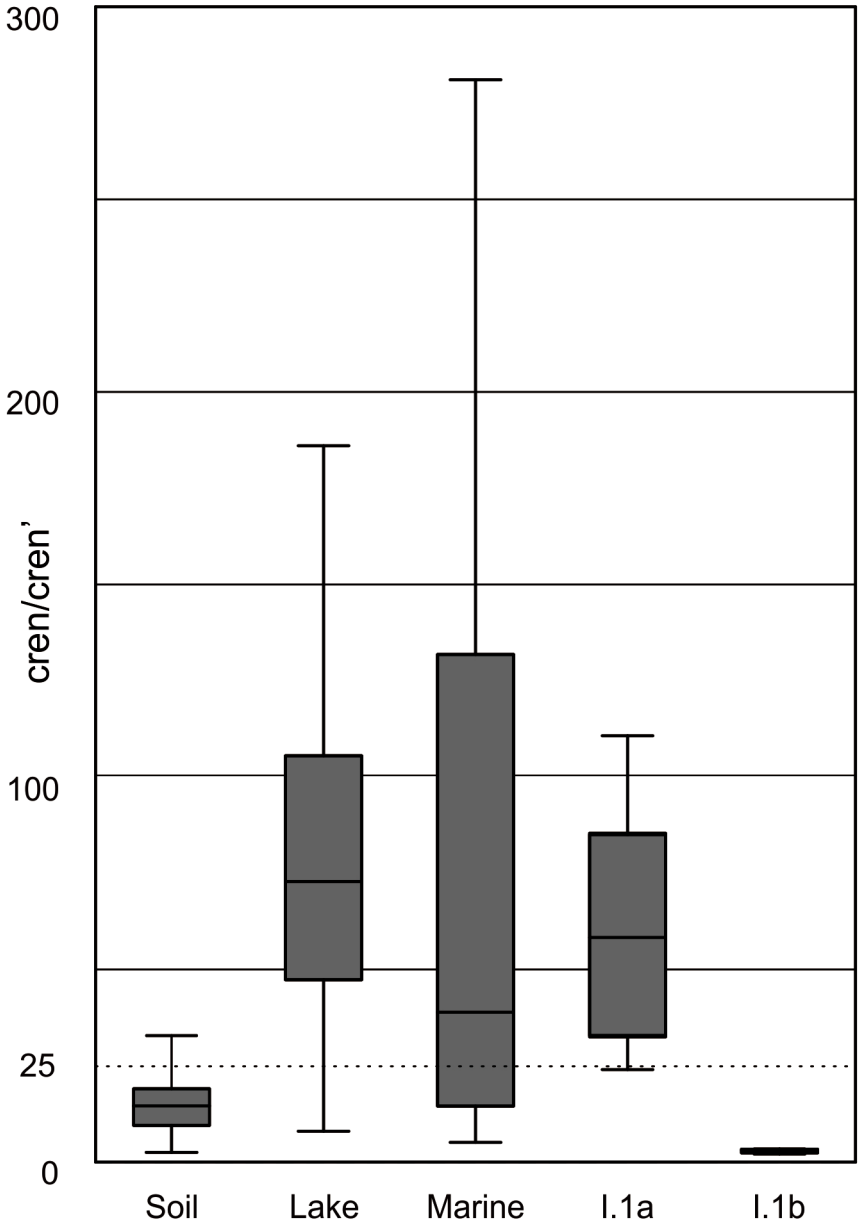


876
877

878 Figure 5

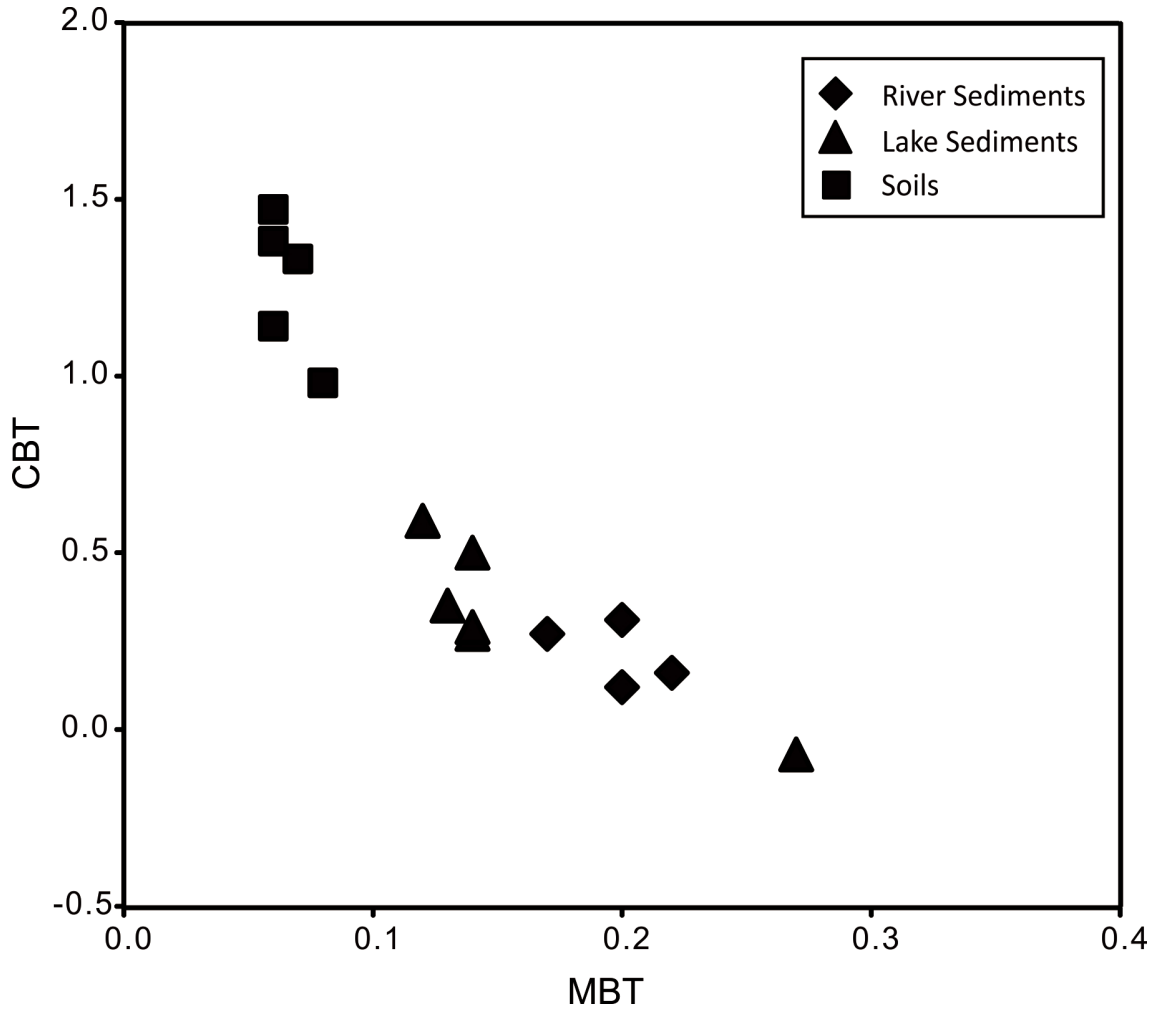


879
880

881

882 Figure 6

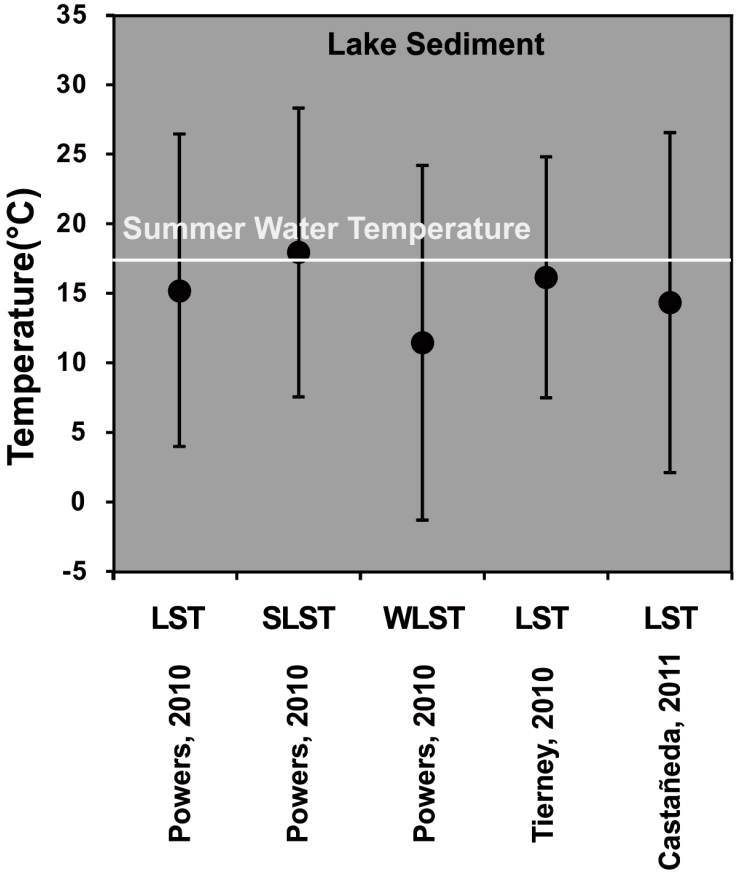


883

884

885

886 Figure 7

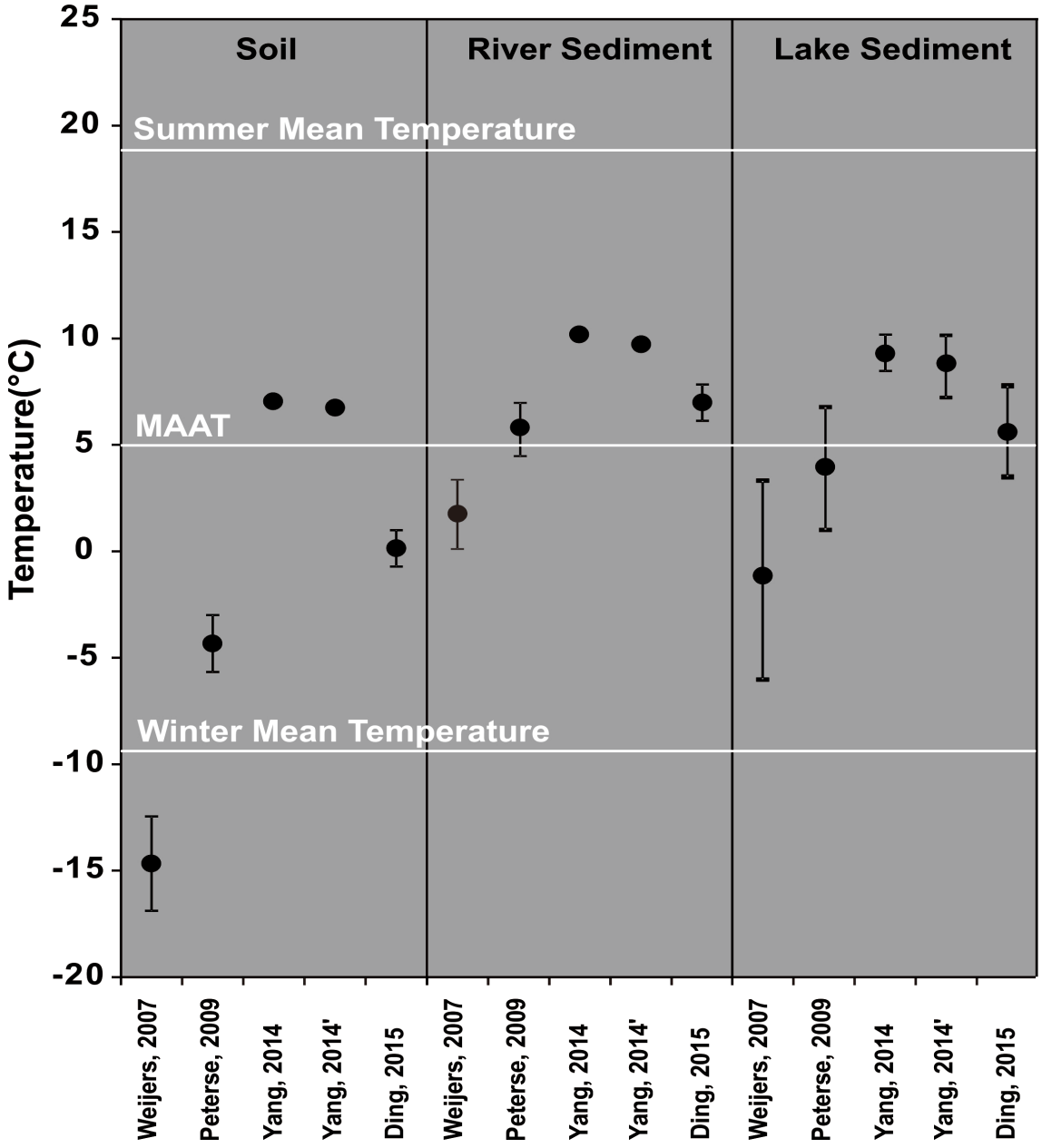


887

888 Figure 8

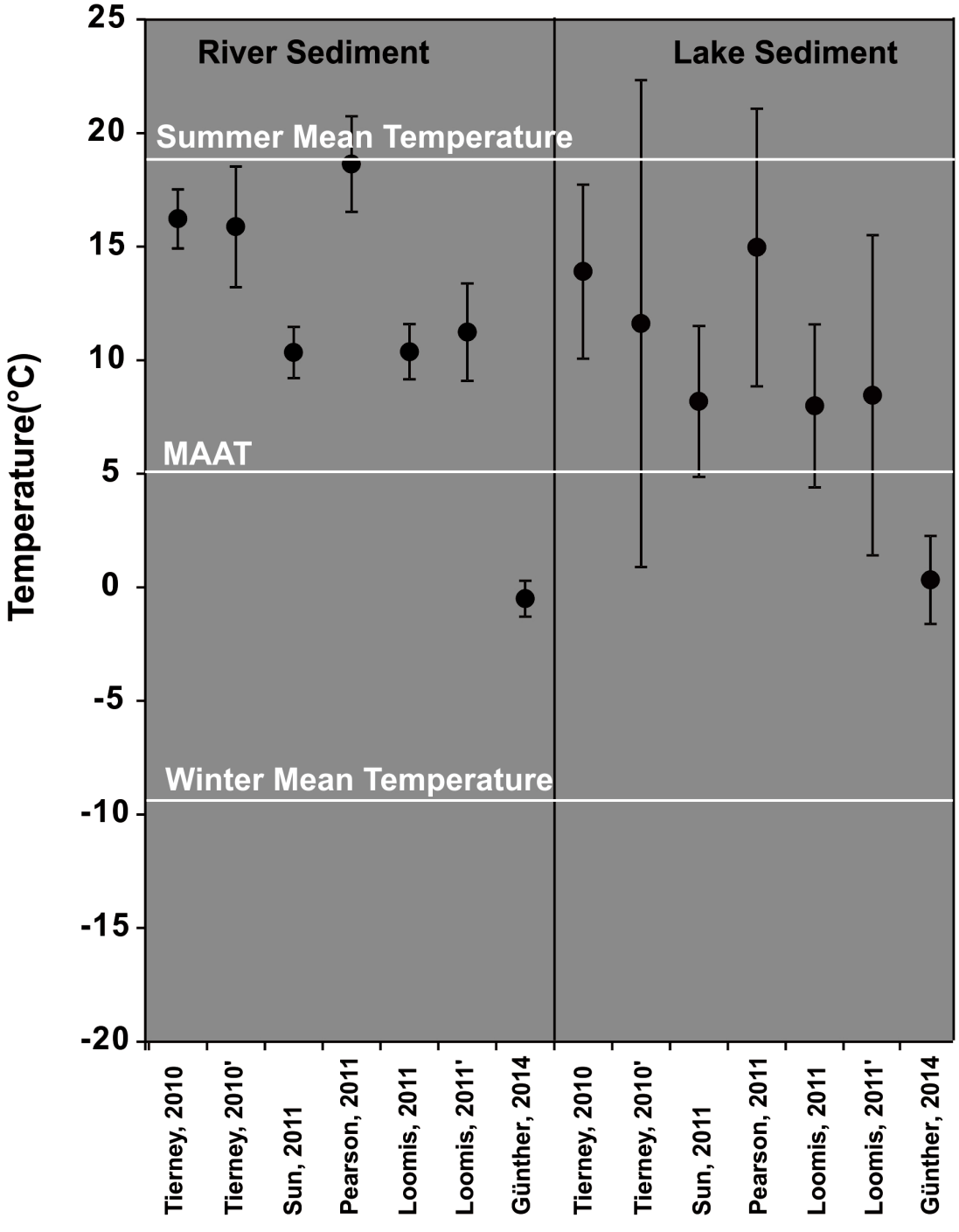


889